# DYNAMICS OF STRUCTURES WITH UNCERTAIN-BUT-BOUNDED PARAMETERS VIA PSEUDO-STATIC SENSITIVITY ANALYSIS

**Giuseppe Muscolino**[a], **Alba Sofi**[b,c,*], **Filippo Giunta**[d]

[a]Department of Engineering and Inter-University Centre of Theoretical and Experimental Dynamics, University of Messina, Villaggio S.Agata, 98166 Messina, Italy, e-mail: gmuscolino@unime.it

[b]Department of Architecture and Territory and Inter-University Centre of Theoretical and Experimental Dynamics, University "Mediterranea" of Reggio Calabria, Salita Melissari, Feo di Vito, 89124 Reggio Calabria Italy, e-mail: alba.sofi@unirc.it

[c]Visiting Fellow, Department of Engineering Science, University of Oxford, Parks Road, Oxford OX1 3PJ, UK

[d]Department of Engineering, University of Messina, Villaggio S.Agata, 98166 Messina, Italy, e-mail: fgiunta@unime.it

## Abstract

This paper deals with the analysis of linear-elastic structures with uncertain-but-bounded parameters subjected to deterministic dynamic loads. A novel procedure based on the use of sensitivity analysis in conjunction with classical modal analysis is proposed. Specifically, a *pseudo-static sensitivity* analysis is performed to seek the combinations of the endpoints of the uncertain parameters which give the lower bound and upper bound of the response at each time instant. Among these, the most common combinations over the time interval of interest are detected in order to avoid the onerous updating of the uncertain parameters at each time instant. Then, the bounds of the response time-history are evaluated by performing two parallel deterministic modal analyses associated to the most common combinations of the extreme values of the interval uncertainties.

Numerical results demonstrate that the proposed method is more efficient than both the *Interval Perturbation Method (IPM)* and classical combinatorial procedure. Furthermore, unlike the *IPM*, it allows the analysis of large-size structures exhibiting relatively large fluctuations of the uncertain parameters.

**Keywords:** Uncertain-but-bounded parameters, interval analysis, interval dynamic structural response, pseudo-static sensitivity, lower and upper bounds of response time-history.

[*]Corresponding author

# 1 INTRODUCTION

It is well known that almost any type of structural systems is subjected to dynamic loads during its lifetime. Typical dangerous dynamic loads may be impulsive (blast or explosion) or long-duration, such as those resulting from earthquakes or wind. A structural dynamic problem differs to a large extent from its static loading counterpart. The main difference lies in the time varying nature of both loading and response. It follows that a dynamic problem does not have a single solution, as in Statics, but a sequence of solutions at each time instant of the response history. While in Statics, algebraic equations are solved to evaluate the response, in Dynamics the problem is governed by *Ordinary Differential Equations* (*ODE*s). Thus, a dynamic analysis is clearly more complex and time-consuming than a static analysis [1].

Furthermore, the main purpose of structural engineering is to evaluate response quantities, such as displacements, rotations, stresses etc., to perform the reliability assessment of a system. To this aim, not only the external loads but also the mechanical properties of structural materials need to be modeled with great accuracy. It has been widely recognized that the latter quantities are affected by uncertainties caused by measurement or manufacturing errors, or other factors. Usually, experimental data available to characterize mechanical material properties are quite limited, so that the probabilistic modeling appears not able to deliver reliable results. Indeed, within a probabilistic framework, the uncertain parameters are modeled as random variables or random fields with assigned probability distribution, under the assumption of knowing complete information to define a probability density function [2]. Furthermore, Ben-Haim and Elishakoff [3] highlighted that even small variations deviating from the real values may cause relatively large errors of the probability distributions in the feasible region of the design space.

Non-probabilistic approaches can be alternatively used to treat uncertainties affecting the mechanical material properties. In this framework, the interval model seems today the most

suitable analytical tool when only range information or tolerance is known [3],[4]. The interval model, which is based on the set theory, represents the uncertain parameters as interval variables with assigned upper and lower bounds without requiring complete information on the distribution of the uncertainties between such bounds.

The main advantage of the *Classical Interval Analysis* (*CIA*) is that it provides analytically rigorous enclosures of the solution [5][6], but its application to practical engineering problems is not an easy task due to two main drawbacks commonly faced in the development of interval-based procedures for structural analysis: *i*) the drastic overestimation of the interval solution range due to the so-called *dependency phenomenon* [2][6]; *ii*) the high computational costs required by uncertainty propagation procedures such as the classical combinatorial approach [2][7].

As stated before, the dynamic equilibrium of linear structural systems is governed by sets of *ODE*s. If the *ODE*s with interval uncertainties are solved using the *CIA*, the overestimation will be accumulated in the process of numerical iterations [8][9]. Several methods have been proposed in literature to limit the overestimation of the solution of the set of *ODE*s governing linear or non-linear dynamic problems with interval uncertainties. In particular, the upper and lower bounds of the dynamic response were obtained by Chen et al. [10] using Taylor series expansion combined with a method based on the matrix perturbation theory. Subsequently, the *Interval Perturbation Method* (*IPM*), which is based on Taylor series expansion and parameter perturbation, has been introduced to evaluate the dynamic response of structures subjected to deterministic [11][14] or stochastic excitations [15]. More recently, Gao et al. [16] presented the *interval factor method* to calculate the dynamic response of truss structures. Rama Rao et al. [17] proposed two methods, the first based on adaptive Taylor series expansion along with gradient method and the second one based on direct optimization, to obtain transient time-history response of structures subjected to a sudden impact load. Yang et al. [18]

used the Laplace transform to convert the *ODE*s into a system of linear equations and the inverse Laplace transform to obtain the time-history response, once the higher-order terms are removed by matrix perturbation technique in Laplace domain. Xia and Yu [19][21] developed a modified *IPM* based on the modified Neumann expansion for the response analysis of interval structures and interval structural-acoustic systems. To handle degrees of uncertainty larger than those allowed by first-order interval Taylor series expansion, Wu et al. [9] introduced Chebyshev series expansions into the interval framework to develop a new method for the analysis of non-linear dynamic systems. Xia et al. [22] proposed a Monte Carlo method based on the Chebyshev polynomial expansion.

Although other methods are more accurate, the *IPM* or, equivalently, the first-order interval Taylor series expansion, is the most widely used to obtain the *lower bound* (*LB*) and *upper bound* (*UB*) of the interval dynamic response. The main advantages of the *IPM* are the flexibility and the simplicity of the mathematical formulation. However, since the effect of neglecting higher-order terms is unpredictable, the effectiveness of this method is limited to uncertainties with small intervals. Furthermore, the computational burden associated to the *IPM* rapidly increases with the dimensions of structural systems and the number of uncertainties.

In this paper, a novel procedure to evaluate the bounds of the interval response of structural systems with uncertain-but-bounded material properties under deterministic dynamic excitations is presented. The key idea of the proposed approach is to properly extend sensitivity-based procedures developed to perform interval static structural analysis [23][24] so as to address dynamic problems. Indeed, at each time instant the dynamic response of a structural system is a monotonic function of the uncertain material properties. In this context, the main issue is the time-dependency of response sensitivities to the uncertain parameters. To overcome this limitation, the present study introduces a *pseudo-static sensitivity* analysis which

involves just the evaluation of the nominal dynamic response time-history. *Pseudo-static sensitivities* provide the combinations of the endpoints of the interval uncertainties to be used to estimate the *LB* and *UB* of the response at each time instant. Then, the issue of time-dependency is bypassed defining just two combinations for estimating the *LB* and *UB* of the response, selected as the most common ones over the time interval of interest. Finally, the bounds of the response time-history can be evaluated by performing two parallel modal analyses associated to the most common combinations of the endpoints of the uncertain parameters. Summarizing, the proposed method requires three main steps: *i*) a preliminary *pseudo-static sensitivity* analysis to define the most common combinations of the endpoints of the interval parameters which give the *LB* and *UB* of the response over the time interval of interest; *ii*) a generalized interval modal analysis which requires the solution of two deterministic eigenproblems associated to the previously defined most common combinations; *iii*) the evaluation of the bounds of the response time-history by performing two parallel step-by-step integrations of the equations of motion in the modal subspace.

Three examples concerning a 3D truss structure, a grid structure and a shell corner under deterministic dynamic excitations are presented. In all the applications, Young' modulus of the material is assumed to be uncertain and the proposed estimates of the bounds of the dynamic response are obtained implementing the presented procedure in the context of the standard finite element method (FEM) exploiting the commercial software ABAQUS. Appropriate comparisons with the exact bounds provided by the classical combinatorial procedure, known as *vertex method* [25], demonstrate that the proposed method, unlike the *IPM*, enables to analyze large structural systems affected by relatively high fluctuations of the uncertain parameters.

The paper is organized as follows: in Section 2, the dynamic problem of structures with uncertain-but-bounded material properties is formulated; Section 3 focuses on the interval free

vibration analysis, with special attention to the solution of the generalized interval eigenproblem; in Section 4, the *pseudo-static sensitivity* analysis of the response is introduced; Section 5 presents a generalized interval modal analysis for the evaluation of the bounds of both free and forced interval vibrations; finally, in Section 6, three numerical applications are provided to demonstrate the accuracy and efficiency of the proposed method.

## 2 PROBLEM STATEMENT

Let us consider a quiescent $n-$DOFs classically damped linear structural system subjected to a deterministic excitation $\mathbf{f}(t)$. The dynamic response of the system is governed by the following set of second-order *Ordinary Differential Equations* (*ODE*s):

$$\mathbf{M}\ddot{\mathbf{u}}(t)+\mathbf{C}\dot{\mathbf{u}}(t)+\mathbf{K}\mathbf{u}(t)=\mathbf{f}(t) \tag{1}$$

where $\mathbf{M}$, $\mathbf{C}$ and $\mathbf{K}$ are the $n\times n$ mass, damping and stiffness matrices of the structure, respectively; $\mathbf{u}(t)$ and $\mathbf{f}(t)$ are $n\times 1$ order time-dependent vectors, collecting the nodal displacements and the external loads, respectively; finally, a dot over a variable denotes differentiation with respect to time $t$. In the following, the Rayleigh model is adopted for the damping matrix.

It is assumed that the mechanical properties of structural material are affected by uncertainties, so that the elements of the stiffness matrix turn out to be uncertain. The dimensionless fluctuation of the $i-$th uncertain property, $d_i^I = d_{0,i}(1+\alpha_i^I)$, around the nominal value, $d_{0,i}$, is modelled as an uncertain-but-bounded parameter, $\alpha_i^I \triangleq \left[\underline{\alpha}_i, \overline{\alpha}_i\right] \in \mathbb{IR}$, with $\mathbb{IR}$ denoting the set of all closed real interval numbers, while $\underline{\alpha}_i$ and $\overline{\alpha}_i$ are the *lower bound* (*LB*) and *upper bound* (*UB*) of $\alpha_i^I$, respectively. Let the structure possess $r$ uncertain

parameters whose fluctuations are collected into the interval vector $\boldsymbol{\alpha}^I = [\alpha_1^I,\ \alpha_2^I,\ \ldots,\ \alpha_r^I]^T$ of order *r*, with the apexes *T* and *I* meaning transpose operator and interval variable, respectively. According to the *Classical Interval Analysis* (*CIA*) [5][6], the *r* uncertain-but-bounded parameters $\alpha_i^I \ \ (i = 1, 2, \ldots, r)$ are assumed to be independent and $\boldsymbol{\alpha}^I \triangleq [\underline{\boldsymbol{\alpha}}, \overline{\boldsymbol{\alpha}}] \in \mathbb{IR}^r$ is a bounded set-interval vector of real numbers such that $\underline{\boldsymbol{\alpha}} \le \boldsymbol{\alpha} \le \overline{\boldsymbol{\alpha}}$, with the symbols $\underline{\boldsymbol{\alpha}}$ and $\overline{\boldsymbol{\alpha}}$ denoting the vectors collecting the *LB* and *UB* of the interval variables $\alpha_i^I$, respectively.

In the framework of interval symbolism, a generic interval-valued function $f$ and a generic interval-valued matrix function $\mathbf{A}$ of the interval vector $\boldsymbol{\alpha}^I$ will be denoted in equivalent form, respectively, as:

$$\begin{aligned} f^I &\equiv f(\boldsymbol{\alpha}^I) \Leftrightarrow f(\boldsymbol{\alpha}), \quad \boldsymbol{\alpha} \in \boldsymbol{\alpha}^I = \left[\underline{\boldsymbol{\alpha}}, \overline{\boldsymbol{\alpha}}\right]; \\ \mathbf{A}^I &\equiv \mathbf{A}(\boldsymbol{\alpha}^I) \Leftrightarrow \mathbf{A}(\boldsymbol{\alpha}), \quad \boldsymbol{\alpha} \in \boldsymbol{\alpha}^I = \left[\underline{\boldsymbol{\alpha}}, \overline{\boldsymbol{\alpha}}\right]. \end{aligned} \tag{2a,b}$$

By taking into account the uncertain mechanical properties, Eq.(1) can be rewritten as:

$$\mathbf{M}\ddot{\mathbf{u}}(\boldsymbol{\alpha}, t) + \mathbf{C}(\boldsymbol{\alpha})\dot{\mathbf{u}}(\boldsymbol{\alpha}, t) + \mathbf{K}(\boldsymbol{\alpha})\mathbf{u}(\boldsymbol{\alpha}, t) = \mathbf{f}(t), \qquad \boldsymbol{\alpha} \in \boldsymbol{\alpha}^I = \left[\underline{\boldsymbol{\alpha}}, \overline{\boldsymbol{\alpha}}\right] \tag{3}$$

where the stiffness matrix $\mathbf{K}(\boldsymbol{\alpha}^I)$ as well as the displacement vector $\mathbf{u}(\boldsymbol{\alpha}^I, t)$ depend on the interval parameters collected into the vector $\boldsymbol{\alpha}^I \triangleq [\underline{\boldsymbol{\alpha}}, \overline{\boldsymbol{\alpha}}] \in \mathbb{IR}^r$. Moreover, since the Rayleigh model is adopted for the damping matrix, the following relationship holds:

$$\mathbf{C}(\boldsymbol{\alpha}) = c_M \mathbf{M} + c_K \mathbf{K}(\boldsymbol{\alpha}), \qquad \boldsymbol{\alpha} \in \boldsymbol{\alpha}^I = \left[\underline{\boldsymbol{\alpha}}, \overline{\boldsymbol{\alpha}}\right] \tag{4}$$

where $c_M$ and $c_K$ are the Rayleigh damping constants having units $s^{-1}$ and $s$, respectively.

Following the *improved interval analysis* (*IIA*) [26], the *i*-th real interval variable $\alpha_i^I$ can be expressed in the following *affine form*

$$\alpha_i^I = \alpha_{0,i} + \Delta\alpha_i \, \hat{e}_i^I, \quad (i = 1,2,...,r) \tag{5}$$

where

$$\alpha_{0,i} = \frac{1}{2}(\underline{\alpha}_i + \overline{\alpha}_i); \quad \Delta\alpha_i = \frac{1}{2}(\overline{\alpha}_i - \underline{\alpha}_i) \tag{6a,b}$$

are the midpoint value (or mean), $\alpha_{0,i}$, and the deviation amplitude (or radius), $\Delta\alpha_i$; $\hat{e}_i^I \triangleq [-1,1]$ is the so-called *Extra Unitary Interval* (*EUI*) [26] associated to the *i*-th real interval variable $\alpha_i^I$.

Since $\alpha_i^I$ denotes the dimensionless fluctuation of the *i*-th uncertain parameter around the nominal value, $d_i^I = d_{0,i}(1+\alpha_i^I)$, it can be reasonably modelled as a symmetric interval variable, that is $\overline{\alpha}_i = -\underline{\alpha}_i \equiv \alpha_i$. Under this assumption, $\alpha_{0,i} = 0$ and $\Delta\alpha_i > 0$, so that Eq. (5) reduces to:

$$\alpha_i^I = \Delta\alpha_i \, \hat{e}_i^I, \quad (i = 1,2,...,r) \tag{7}$$

where $\Delta\alpha_i < 1$ in order to ensure always positive values of the uncertain physical properties.

Following the interval formalism above introduced, the interval stiffness matrix $\mathbf{K}(\boldsymbol{\alpha}^I)$ can be expressed as:

$$\mathbf{K}(\boldsymbol{\alpha}) = \mathbf{K}_0 + \Delta\mathbf{K}(\boldsymbol{\alpha}); \quad \boldsymbol{\alpha} \in \boldsymbol{\alpha}^I = [\underline{\boldsymbol{\alpha}}, \overline{\boldsymbol{\alpha}}] \tag{8}$$

where $\mathbf{K}_0$ is the nominal stiffness matrix, which is a positive-definite symmetric matrix of order $n \times n$ pertaining to the structure with $\boldsymbol{\alpha} = \mathbf{0}$, and $\Delta\mathbf{K}(\boldsymbol{\alpha}^I)$ is the interval deviation of the stiffness matrix with respect to the nominal one.

At each time instant, all possible solutions of the equations of motion obtained as the uncertain parameters $\alpha_i^I$ (see Eq. (7)) vary independently over their ranges are contained within a solution set:

$$\Sigma(t) = \left\{ \mathbf{u}(\boldsymbol{\alpha},t) \in \mathbb{R}^n \middle| \mathbf{M}\,\ddot{\mathbf{u}}(\boldsymbol{\alpha},t) + \mathbf{C}(\boldsymbol{\alpha})\,\dot{\mathbf{u}}(\boldsymbol{\alpha},t) + \mathbf{K}(\boldsymbol{\alpha})\,\mathbf{u}(\boldsymbol{\alpha},t) = \mathbf{f}(t), \quad \boldsymbol{\alpha} \in \boldsymbol{\alpha}^I = \left[\underline{\boldsymbol{\alpha}}, \overline{\boldsymbol{\alpha}}\right] \right\} \tag{9}$$

where $\left\{ S(\boldsymbol{\alpha},t) \middle| P(\boldsymbol{\alpha},t) \right\}$ means "the set of quantities $S(\boldsymbol{\alpha},t)$ such that the proposition $P(\boldsymbol{\alpha},t)$ holds".

As known, the exact evaluation of the solution set is very difficult, especially in the presence of dynamic excitations. Therefore, within the interval framework, the solution of Eq. (3) is carried out by seeking, at each time instant, the *LB* and *UB* of the interval displacement vector, containing the solution set, which has the narrowest interval components, i.e.

$$\mathbf{u}(\boldsymbol{\alpha}^I,t) = \left[\underline{\mathbf{u}}(t), \overline{\mathbf{u}}(t)\right] \tag{10}$$

or in component form

$$u_j(\boldsymbol{\alpha}^I,t) = \left[\underline{u}_j(t), \overline{u}_j(t)\right], \quad (j = 1,2,\ldots,n) \tag{11}$$

with

$$\begin{aligned} \underline{u}_j(t) &= \min\left\{ u_j(\boldsymbol{\alpha},t) \middle| \; u_j(\boldsymbol{\alpha},t) \in \mathbb{R}, \boldsymbol{\alpha} \in \mathbb{IR}^r \right\}, \\ \overline{u}_j(t) &= \max\left\{ u_j(\boldsymbol{\alpha},t) \middle| \; u_j(\boldsymbol{\alpha},t) \in \mathbb{R}, \boldsymbol{\alpha} \in \mathbb{IR}^r \right\}, \quad (j = 1,2,\ldots,n) \end{aligned} \tag{12a,b}$$

where the symbols $\min\{\bullet\}$ and $\max\{\bullet\}$ mean minimum (inferior) and maximum (superior) value of the quantity between parentheses.

## 3 INTERVAL FREE VIBRATIONS

This section focuses on the formulation of the interval free vibration problem. Let $\mathbf{z}(\boldsymbol{\alpha},t)$ denote the $2n$-order interval vector of state variables, defined as:

$$\mathbf{z}(\boldsymbol{\alpha},t)=\begin{bmatrix}\mathbf{u}(\boldsymbol{\alpha},t)\\ \dot{\mathbf{u}}(\boldsymbol{\alpha},t)\end{bmatrix},\qquad \boldsymbol{\alpha}\in\boldsymbol{\alpha}^I=\left[\underline{\boldsymbol{\alpha}},\overline{\boldsymbol{\alpha}}\right]. \tag{13}$$

Then, the equations of motion (3) can be rewritten in the following form:

$$\dot{\mathbf{z}}(\boldsymbol{\alpha},t)=\mathbf{D}_{\mathrm{N}}(\boldsymbol{\alpha})\,\mathbf{z}(\boldsymbol{\alpha},t)+\mathbf{V}_{\mathrm{N}}\mathbf{f}(t),\qquad \boldsymbol{\alpha}\in\boldsymbol{\alpha}^I=\left[\underline{\boldsymbol{\alpha}},\overline{\boldsymbol{\alpha}}\right] \tag{14}$$

where

$$\mathbf{D}_{\mathrm{N}}(\boldsymbol{\alpha})=\begin{bmatrix}\mathbf{0} & \mathbf{I}_n\\ -\mathbf{M}^{-1}\mathbf{K}(\boldsymbol{\alpha}) & -\mathbf{M}^{-1}\mathbf{C}(\boldsymbol{\alpha})\end{bmatrix};\qquad \mathbf{V}_{\mathrm{N}}=\begin{bmatrix}\mathbf{0}\\ \mathbf{M}^{-1}\end{bmatrix} \tag{15a,b}$$

$\mathbf{I}_n$ denotes the identity matrix of order $n$ and $\mathbf{0}$ the zero matrix; the subscript N means nodal space. The set of first-order *ODE*s (14) represents the equations of motion in the nodal state variable space of the structural system with uncertain parameters collected into the interval vector $\boldsymbol{\alpha}\in\boldsymbol{\alpha}^I=\left[\underline{\boldsymbol{\alpha}},\overline{\boldsymbol{\alpha}}\right]$. In this space, the solution of the free vibration problem, evaluated setting $\mathbf{f}(t)=\mathbf{0}$, is given by the following relationship [27][28]:

$$\mathbf{z}(\boldsymbol{\alpha},t)=\boldsymbol{\Theta}_{\mathrm{N}}(\boldsymbol{\alpha},t-t_0)\,\mathbf{z}(\boldsymbol{\alpha},t_0)\,\mathcal{U}(t-t_0),\qquad \boldsymbol{\alpha}\in\boldsymbol{\alpha}^I=\left[\underline{\boldsymbol{\alpha}},\overline{\boldsymbol{\alpha}}\right] \tag{16}$$

where $\mathbf{z}(\boldsymbol{\alpha},t_0)$ is the state variable vector listing the initial conditions at the time instant $t_0$ and $\mathcal{U}(t)$ is the *unit step function*, defined as

$$\mathcal{U}(t-t_0)=\begin{cases}0, & t\le t_0;\\ 1, & t>t_0.\end{cases} \tag{17}$$

In Eq.(16), $\boldsymbol{\Theta}_{\mathrm{N}}(\boldsymbol{\alpha}^I,t)=\exp\left[\mathbf{D}_{\mathrm{N}}(\boldsymbol{\alpha}^I)\,t\right]$ is the *interval transition matrix* which, for classically damped systems, can be evaluated by interval extension as [27]:

$$\boldsymbol{\Theta}_{\mathrm{N}}(\boldsymbol{\alpha},t)=\begin{bmatrix}-\boldsymbol{\Phi}(\boldsymbol{\alpha})\mathbf{g}(\boldsymbol{\alpha},t)\boldsymbol{\Phi}^{T}(\boldsymbol{\alpha})\mathbf{K}(\boldsymbol{\alpha}) & \boldsymbol{\Phi}(\boldsymbol{\alpha})\dot{\mathbf{g}}(\boldsymbol{\alpha},t)\boldsymbol{\Phi}^{T}(\boldsymbol{\alpha})\mathbf{M}\\ -\boldsymbol{\Phi}(\boldsymbol{\alpha})\dot{\mathbf{g}}(\boldsymbol{\alpha},t)\boldsymbol{\Phi}^{T}(\boldsymbol{\alpha})\mathbf{K}(\boldsymbol{\alpha}) & \boldsymbol{\Phi}(\boldsymbol{\alpha})\ddot{\mathbf{g}}(\boldsymbol{\alpha},t)\boldsymbol{\Phi}^{T}(\boldsymbol{\alpha})\mathbf{M}\end{bmatrix},\quad \boldsymbol{\alpha}\in\boldsymbol{\alpha}^{I}=\left[\underline{\boldsymbol{\alpha}},\overline{\boldsymbol{\alpha}}\right]. \tag{18}$$

Furthermore, it is observed that the response decreases with time because the transition matrix satisfies the following condition:

$$\lim_{t\to\infty}\boldsymbol{\Theta}_{\mathrm{N}}(\boldsymbol{\alpha}^{I},t)=\mathbf{0}. \tag{19}$$

In Eq.(18), $\mathbf{g}\left(\boldsymbol{\alpha}^{I},t\right)$ is an interval diagonal matrix whose *j*-th element can be evaluated as:

$$g_{j}\left(\boldsymbol{\alpha},t\right)=-\exp\left[-\xi_{j}(\boldsymbol{\alpha})\sqrt{\lambda_{j}(\boldsymbol{\alpha})}t\right]\left[\frac{\cos\left(t\sqrt{\lambda_{j}(\boldsymbol{\alpha})\left(1-\xi_{j}^{2}(\boldsymbol{\alpha})\right)}\right)}{\lambda_{j}(\boldsymbol{\alpha})}+\frac{\xi_{j}(\boldsymbol{\alpha})\,\mathrm{sen}\left(t\sqrt{\lambda_{j}(\boldsymbol{\alpha})\left(1-\xi_{j}^{2}(\boldsymbol{\alpha})\right)}\right)}{\lambda_{j}(\boldsymbol{\alpha})\sqrt{1-\xi_{j}^{2}(\boldsymbol{\alpha})}}\right],\quad \boldsymbol{\alpha}\in\boldsymbol{\alpha}^{I}=\left[\underline{\boldsymbol{\alpha}},\overline{\boldsymbol{\alpha}}\right] \tag{20}$$

where $\xi_{j}(\boldsymbol{\alpha})=(c_{M}+c_{K}\,\lambda_{j}(\boldsymbol{\alpha}))\big/2\sqrt{\lambda_{j}(\boldsymbol{\alpha})}$ is the $j-$th interval damping ratio under the Rayleigh condition (4). In the previous equations, $\boldsymbol{\Phi}\left(\boldsymbol{\alpha}^{I}\right)=\left[\begin{array}{cccc}\boldsymbol{\phi}_{1}(\boldsymbol{\alpha}^{I}) & \boldsymbol{\phi}_{2}(\boldsymbol{\alpha}^{I}) & \cdots & \boldsymbol{\phi}_{n}(\boldsymbol{\alpha}^{I})\end{array}\right]$ is the interval modal matrix whose $k-$th column, $\boldsymbol{\phi}_{k}(\boldsymbol{\alpha}^{I})$, is the interval eigenvector associated to the $k-$th interval eigenvalue, $\lambda_{k}(\boldsymbol{\alpha}^{I})=\omega_{k}^{2}(\boldsymbol{\alpha}^{I})$, equivalent to the squared interval natural frequency, solution of the following eigenproblem:

$$\mathbf{K}(\boldsymbol{\alpha})\boldsymbol{\phi}_{k}(\boldsymbol{\alpha})=\lambda_{k}(\boldsymbol{\alpha})\mathbf{M}\boldsymbol{\phi}_{k}(\boldsymbol{\alpha}),\quad \boldsymbol{\alpha}\in\boldsymbol{\alpha}^{I}=\left[\underline{\boldsymbol{\alpha}},\overline{\boldsymbol{\alpha}}\right],\quad (k=1,2,\ldots,n). \tag{21}$$

The solution of this interval eigenvalue problem involves the evaluation of all possible eigenvalues satisfying Eq. (21) as the uncertain parameters assume all possible values inside the interval $\boldsymbol{\alpha}^{I}=\left[\underline{\boldsymbol{\alpha}},\overline{\boldsymbol{\alpha}}\right]$. The solutions constitute a complicated region in the real number field $\mathbb{R}$. Recently, it has been shown that, since the eigenvalues are monotonic functions of the uncer-

tain parameters $\alpha_j \in \alpha_j^I = \left[\underline{\alpha}_j, \overline{\alpha}_j\right]$, $(j = 1,2,\ldots,r)$, the narrowest interval enclosing all possible eigenvalues can be obtained by solving the following two deterministic eigenproblems [29][32]:

$$\begin{aligned} &\mathbf{K}\left(\underline{\boldsymbol{\alpha}}\right)\boldsymbol{\phi}_k^{(\mathrm{LB})} = \underline{\lambda}_k\, \mathbf{M}\boldsymbol{\phi}_k^{(\mathrm{LB})}; \quad \boldsymbol{\phi}_k^{(\mathrm{LB})T}\, \mathbf{M}\boldsymbol{\phi}_\ell^{(\mathrm{LB})} = \Delta_{k\ell} \\ &\mathbf{K}\left(\overline{\boldsymbol{\alpha}}\right)\boldsymbol{\phi}_k^{(\mathrm{UB})} = \overline{\lambda}_k\, \mathbf{M}\boldsymbol{\phi}_k^{(\mathrm{UB})}; \quad \boldsymbol{\phi}_k^{(\mathrm{UB})T}\, \mathbf{M}\boldsymbol{\phi}_\ell^{(\mathrm{LB})} = \Delta_{k\ell}, \quad (j = 1,2,\ldots n) \end{aligned} \tag{22a,b}$$

where $\Delta_{jk}$ is the Kronecker delta; $\boldsymbol{\phi}_k^{(\mathrm{LB})}$ and $\boldsymbol{\phi}_k^{(\mathrm{UB})}$ $(k = 1,2,\ldots,n)$ are the eigenvectors solution of the eigenproblem (22a) and (22b) in which $\boldsymbol{\alpha} = \underline{\boldsymbol{\alpha}}$ and $\boldsymbol{\alpha} = \overline{\boldsymbol{\alpha}}$, respectively; while $\underline{\lambda}_k$ and $\overline{\lambda}_k$, $(k = 1,2,\ldots,n)$, are the *LB* and *UB* of the $k-$th interval eigenvalue. By inspection of the eigenproblems (22a,b), it appears that the narrowest interval for each eigenvalue corresponds to the so-called *trivial* combinations of the endpoints of the uncertain-but-bounded parameters. In fact, the *LB*s and *UB*s of each eigenvalue are obtained when all the interval fluctuations $\alpha_j \in \alpha_j^I = \left[\underline{\alpha}_j, \overline{\alpha}_j\right]$, $(j = 1,2,\ldots,r)$, are set simultaneously to their *LB*s or *UB*s, respectively. However, it is well known that the narrowest interval of the dynamic response commonly corresponds to combinations of the extreme values of the uncertain parameters different from the *trivial* ones. Hence, a modal analysis based on the narrowest set of eigenvalues, solutions of Eqs.(22a,b), often does not guarantee the narrowest interval of the response time-history. For this reason, in the next sections, an alternative method will be presented. The proposed method basically requires the following three steps: *i*) a preliminary *pseudo-static sensitivity analysis* to define the most common combinations of the endpoints of the interval parameters to be used for estimating the *LB* and *UB* of the response over the whole time history; *ii*) a generalized interval modal analysis which requires the solution of two deterministic eigenproblems and the step-by-step integration of two deterministic equations of motion in the modal sub-space corresponding to the most common combinations defined in the pre-

vious step; *iii*) the evaluation of the *LB* and *UB* of the response time-history by seeking, at each time instant, the minimum and maximum, respectively, among the responses pertaining to the most common combinations.

## 4 PSEUDO-STATIC SENSITIVITY ANALYSIS

The interval sensitivity analysis of structural systems should quantify the impact of the change of an individual interval parameter on the generic output quantity of interest (displacement, rotation, stress etc.). Generally, it represents the degree of influence of the width of each uncertain-but-bounded structural parameter on the width of the output interval [2][33]. Moreover, since in structural engineering the response quantities are monotonic functions of the uncertain parameters, sensitivity-based approaches have been developed within a static setting to evaluate the approximate bound values of the response by using appropriate end-points of the intervals [23][24]. The main objective of this section is to extend such well-established sensitivity-based procedures to evaluate the approximate time-dependent bound functions of the interval dynamic response. To this aim, first the definition of *pseudo-static sensitivity* function of the dynamic response with respect to the uncertain parameters is introduced. As an example, the vector collecting the *pseudo-static sensitivity* functions of the displacement time-history with respect to the $\ell$-th uncertain parameter, $\alpha_\ell \in \alpha_\ell^I = \left[\underline{\alpha}_\ell, \overline{\alpha}_\ell\right]$, is defined by the following explicit expression:

$$\mathbf{s}_{\mathbf{u},\ell}(t) = \left.\frac{\partial \mathbf{u}(\boldsymbol{\alpha}, t)}{\partial \alpha_\ell}\right|_{\boldsymbol{\alpha}=\mathbf{0}} = -\mathbf{K}_0^{-1}\mathbf{K}_\ell \mathbf{u}_0(t), \quad (\ell = 1, 2, \ldots, r) \tag{23}$$

where $\mathbf{u}_0(t)$ is the nominal displacement vector, i.e. for $\boldsymbol{\alpha} = \mathbf{0}$, and $\mathbf{K}_\ell$ is a semi-definite positive matrix given by:

$$\mathbf{K}_\ell = \left.\frac{\partial \mathbf{K}(\boldsymbol{\alpha})}{\partial \alpha_\ell}\right|_{\boldsymbol{\alpha}=\mathbf{0}} . \tag{24}$$

Equation (23) is obtained by direct differentiating the equations of motion (3) and then neglecting inertial and damping terms. Within the dynamic framework, the $j$-th component, $s_{u_j,\ell}(t)$, of the *pseudo-static sensitivity* vector function, $\mathbf{s}_{\mathbf{u},\ell}(t)$, defined in Eq. (23), at each time instant, gives information about the change of the displacement $u_j(\boldsymbol{\alpha}^I, t)$ due to a variation of the $\ell$-th structural parameter $\alpha_\ell \in \alpha_\ell^I = \left[\underline{\alpha}_\ell, \overline{\alpha}_\ell\right]$ with respect to the nominal value. Specifically, within a small range around $\boldsymbol{\alpha} = \mathbf{0}$, at each time instant, $u_j(\boldsymbol{\alpha}^I, t)$ is an increasing or decreasing function of the parameter $\alpha_\ell$ depending on whether $s_{u_j,\ell}(t) > 0$ or $s_{u_j,\ell}(t) < 0$, respectively.

The nominal displacement vector $\mathbf{u}_0(t)$ in Eq.(23) is ruled by the following set of second-order *ODE*s:

$$\mathbf{M}\ddot{\mathbf{u}}_0(t) + \mathbf{C}_0\dot{\mathbf{u}}_0(t) + \mathbf{K}_0\mathbf{u}_0(t) = \mathbf{f}(t) \tag{25}$$

with $\mathbf{C}_0 = c_M\mathbf{M} + c_K\mathbf{K}_0$. The solution of Eq. (25) can be performed by classical modal analysis. To this aim, the following coordinate transformation is introduced:

$$\mathbf{u}_0(t) = \boldsymbol{\Phi}_0\mathbf{q}_0(t) \tag{26}$$

where $\boldsymbol{\Phi}_0$ is a matrix of order $n \times m$ ($m \le n$ being a suitable integer) collecting the first $m$ eigenvectors, normalized with respect to the mass matrix $\mathbf{M}$, solution of the following eigenproblem:

$$\mathbf{K}_0\boldsymbol{\Phi}_0 = \mathbf{M}\boldsymbol{\Phi}_0\boldsymbol{\Omega}_0^2; \quad \boldsymbol{\Phi}_0^T\mathbf{M}\boldsymbol{\Phi}_0 = \mathbf{I}_m \tag{27}$$

in which $\mathbf{I}_m$ is the identity matrix of order $m$; $\mathbf{\Phi}_0$ and $\mathbf{\Omega}_0$ are the modal matrix and a diagonal matrix of order *m* listing the first *m* natural circular frequencies, $\omega_{0,k}$, of the structural system with nominal values of the uncertain parameters, respectively. By applying the coordinate transformation in Eq. (26) to Eq.(25), the following set of decoupled second-order *ODE*s in the modal subspace is obtained:

$$\ddot{\mathbf{q}}_0(t) + \mathbf{\Xi}_0\, \dot{\mathbf{q}}_0(t) + \mathbf{\Omega}_0\, \mathbf{q}_0(t) = \mathbf{\Phi}_0^T\, \mathbf{f}(t) \tag{28}$$

with $\mathbf{\Xi}_0 = c_M\, \mathbf{I}_m + c_K\, \mathbf{\Omega}_0$.

Let the combinations of the extreme values of the $\ell$-th uncertain parameter providing the *LB* and *UB* of the $j$-th displacement component $u_j(\boldsymbol{\alpha}^I, t)$ at the time instant $t$ be denoted by $\alpha_{j,\ell}^{(\mathrm{LB})}(t)$ and $\alpha_{j,\ell}^{(\mathrm{UB})}(t)$, respectively. Based on the knowledge of the *pseudo-static sensitivity* functions $s_{u_j,\ell}$, $(\ell = 1,2,\ldots,r)$, such combinations can be estimated as follows:

$$\begin{aligned}
&\text{if} \quad s_{u_j,\ell}(t) > 0, \quad \text{then} \quad \alpha_{j,\ell}^{(\mathrm{UB})}(t) = \overline{\alpha}_\ell(t), \quad \alpha_{j,\ell}^{(\mathrm{LB})}(t) = \underline{\alpha}_\ell(t); \\
&\text{if} \quad s_{u_j,\ell}(t) < 0, \quad \text{then} \quad \alpha_{j,\ell}^{(\mathrm{UB})}(t) = \underline{\alpha}_\ell(t), \quad \alpha_{j,\ell}^{(\mathrm{LB})}(t) = \overline{\alpha}_\ell(t), \\
&\qquad\qquad\qquad\qquad\qquad\qquad (j = 1,2,\ldots,n; \;\; \ell = 1,2,\ldots,r).
\end{aligned} \tag{29a,b}$$

The functions $\alpha_{j,\ell}^{(\mathrm{LB})}(t)$ and $\alpha_{j,\ell}^{(\mathrm{UB})}(t)$ can be collected into the following time-dependent vectors of order *r*:

$$\begin{aligned}
\boldsymbol{\alpha}_j^{(\mathrm{LB})}(t) &= \left[\, \alpha_{j,1}^{(\mathrm{LB})}(t) \quad \alpha_{j,2}^{(\mathrm{LB})}(t) \quad \ldots \quad \alpha_{j,r}^{(\mathrm{LB})}(t) \,\right]^T; \\
\boldsymbol{\alpha}_j^{(\mathrm{UB})}(t) &= \left[\, \alpha_{j,1}^{(\mathrm{UB})}(t) \quad \alpha_{j,2}^{(\mathrm{UB})}(t) \quad \ldots \quad \alpha_{j,r}^{(\mathrm{UB})}(t) \,\right]^T, \quad (j = 1,2,\ldots,n).
\end{aligned} \tag{30a,b}$$

Compared to the static case [23][24], the main difficulty in the application of the sensitivity-based approach to dynamic problems lies in the fact that the above defined combinations of the endpoints of the interval parameters are time-dependent ones. This implies that, to ob-

tain the approximate *LB* and *UB* of the interval dynamic displacement component $u_j(\boldsymbol{\alpha}^I,t)$, the equations of motion of the structural system have to be integrated by a step-by-step algorithm replacing at each time step the values of the uncertain parameters collected into the vectors $\boldsymbol{\alpha}_j^{(\mathrm{LB})}(t)$ and $\boldsymbol{\alpha}_j^{(\mathrm{LB})}(t)$ (see Eqs. (30a,b)), respectively. It can be readily inferred that this procedure is very cumbersome and requires high computational effort.

An efficient way to overcome this drawback is to find two combinations of the endpoints of the uncertain parameters which do not vary with time and give accurate estimates of the *LB* and *UB* of the response time-history. The key idea of the proposed approach is to define such combinations as the most common among the combinations deduced over the whole time interval of interest based on the information provided by the above described *pseudo-static sensitivity* analysis. These combinations are collected in the time independent vectors $\underset{\sim}{\boldsymbol{\alpha}}_{\mathrm{C},j}$ and $\tilde{\boldsymbol{\alpha}}_{\mathrm{C},j}$, which can be evaluated simply by using the built-in function "Commonest" of Wolfram Mathematica, that is:

$$\underset{\sim}{\boldsymbol{\alpha}}_{\mathrm{C},j}=\begin{bmatrix}\underset{\sim}{\alpha}_{C,j,1} & \underset{\sim}{\alpha}_{C,j,2} & \dots & \underset{\sim}{\alpha}_{C,j,r}\end{bmatrix}^T=\underset{0<t\le t_F}{\mathrm{Commonest}}\left\{\alpha_{j,1}^{(\mathrm{LB})}(t) \quad \alpha_{j,2}^{(\mathrm{LB})}(t) \quad \dots \quad \alpha_{j,r}^{(\mathrm{LB})}(t)\right\};$$

$$\tilde{\boldsymbol{\alpha}}_{\mathrm{C},j}=\begin{bmatrix}\tilde{\alpha}_{C,j,1} & \tilde{\alpha}_{C,j,2} & \dots & \tilde{\alpha}_{C,j,r}\end{bmatrix}^T=\underset{0<t\le t_F}{\mathrm{Commonest}}\left\{\alpha_{j,1}^{(\mathrm{UB})}(t) \quad \alpha_{j,2}^{(\mathrm{UB})}(t) \quad \dots \quad \alpha_{j,r}^{(\mathrm{UB})}(t)\right\},\quad (j=1,2,\dots,n)$$

(31a,b)

where $0<t\le t_F$ is the time interval of interest. In the previous equations, $\underset{\sim}{\boldsymbol{\alpha}}_{\mathrm{C},j}$ and $\tilde{\boldsymbol{\alpha}}_{\mathrm{C},j}$ collect the most common extreme values of the uncertain parameters which, according to *pseudo-static sensitivity* analysis, provide the *LB* and *UB* of the displacement $u_j(\boldsymbol{\alpha}^I,t)$, respectively, over the time interval $0<t\le t_F$.

## 5 GENERALIZED INTERVAL MODAL ANALYSIS

As known, the main step in vibration analysis of structures is the evaluation of the natural frequencies and associated mode shapes to apply the classical modal analysis which, for classically damped linear systems, leads to a set of decoupled second-order *ODE*s. However, as already mentioned, a modal analysis based on the narrowest set of eigenvalues, solutions of Eqs.(22a,b), corresponding to the so-called *trivial* combinations of the endpoints of the uncertain parameters, does not always guarantee the narrowest interval of the time-history response. Indeed, numerical investigations on several structural systems have shown that the most common combinations provided by the *pseudo-static sensitivity* analysis (see Section 4) are often quite different from the *trivial* ones. Then, the idea is to perform a generalized interval modal analysis associated to the most common combinations of the endpoints of the interval parameters (see Eqs. (31a,b)). To this aim, the following two deterministic eigenvalue problems are solved:

$$\begin{aligned} &\mathbf{K}\left(\underset{\sim}{\boldsymbol{\alpha}}_{\mathrm{C},j}\right)\underset{\sim}{\boldsymbol{\phi}}_{j,k} = \underset{\sim}{\lambda}_{j,k}\,\mathbf{M}\,\underset{\sim}{\boldsymbol{\phi}}_{j,k}\;; \quad \underset{\sim}{\boldsymbol{\phi}}_{j,k}^{T}\,\mathbf{M}\,\underset{\sim}{\boldsymbol{\phi}}_{j,\ell} = \Delta_{k\ell} \\ &\mathbf{K}\left(\tilde{\boldsymbol{\alpha}}_{\mathrm{C},j}\right)\tilde{\boldsymbol{\phi}}_{j,k} = \tilde{\lambda}_{j,k}\,\mathbf{M}\,\tilde{\boldsymbol{\phi}}_{j,k}; \quad \tilde{\boldsymbol{\phi}}_{j,k}^{T}\,\mathbf{M}\,\tilde{\boldsymbol{\phi}}_{j,\ell} = \Delta_{k\ell}\,, \quad (j,k,\ell = 1,2,\ldots n) \end{aligned} \tag{32a,b}$$

where $\underset{\sim}{\boldsymbol{\alpha}}_{\mathrm{C},j}$ and $\tilde{\boldsymbol{\alpha}}_{\mathrm{C},j}$ are the vectors collecting the most common combinations defined in Eqs.(31a,b) to evaluate the approximate *LB* and *UB* of the time-history of the *j*-th displacement component, respectively; $\underset{\sim}{\lambda}_{j,k}$ and $\underset{\sim}{\boldsymbol{\phi}}_{j,k}$ are the *k*-th eigenvalue and eigenvector, solution of the eigenproblem in Eq. (32a) corresponding to $\boldsymbol{\alpha} = \underset{\sim}{\boldsymbol{\alpha}}_{\mathrm{C},j}$; $\tilde{\lambda}_{j,k}$ and $\tilde{\boldsymbol{\phi}}_{j,k}$ are the *k*-th eigenvalue and eigenvector, solution of the eigenproblem in Eq. (32b) corresponding to $\boldsymbol{\alpha} = \tilde{\boldsymbol{\alpha}}_{\mathrm{C},j}$. Notice that, since the two stiffness matrices $\mathbf{K}(\underset{\sim}{\boldsymbol{\alpha}}_{\mathrm{C},j})$ and $\mathbf{K}(\tilde{\boldsymbol{\alpha}}_{\mathrm{C},j})$ as well as the mass matrix $\mathbf{M}$ are real, symmetric and positive-definite matrices, the eigenvectors solution of both eigenproblems are real vectors, while the eigenvalues are real and positive quantities.

Once the eigenproperties are evaluated, the time-histories of the $j$-th displacement component corresponding to $\boldsymbol{\alpha} = \tilde{\boldsymbol{\alpha}}_{\mathrm{C},j}$ and $\boldsymbol{\alpha} = \underset{\sim}{\boldsymbol{\alpha}}_{\mathrm{C},j}$ can be evaluated by classical modal analysis performing the following two coordinate transformations:

$$\begin{aligned} \underset{\sim}{u}_j(t) &\equiv u_j(\underset{\sim}{\boldsymbol{\alpha}}_{\mathrm{C},j}, t) = \sum_{k=1}^{m} \underset{\sim}{\phi}_{j,jk}\, \underset{\sim}{q}_{j,k}(t); \\ \tilde{u}_j(t) &\equiv u_j(\tilde{\boldsymbol{\alpha}}_{\mathrm{C},j}, t) = \sum_{k=1}^{m} \tilde{\phi}_{j,jk}\, \tilde{q}_{j,k}(t) \end{aligned} \tag{33a,b}$$

where $m$ is the number of retained modes; $\underset{\sim}{\phi}_{j,jk}$ and $\tilde{\phi}_{j,jk}$ are the $j$-th elements of the eigenvectors $\underset{\sim}{\boldsymbol{\phi}}_{j,k}$ and $\tilde{\boldsymbol{\phi}}_{j,k}$, respectively; $\underset{\sim}{q}_{j,k}(t)$ and $\tilde{q}_{j,k}(t)$ denote the $k-$th time-dependent modal coordinates associated to the most common combinations of the endpoints of the uncertain parameters, $\boldsymbol{\alpha} = \tilde{\boldsymbol{\alpha}}_{\mathrm{C},j}$ and $\boldsymbol{\alpha} = \underset{\sim}{\boldsymbol{\alpha}}_{\mathrm{C},j}$, to be used for the evaluation of the *UB* and *LB* of the interval displacement $u_j^I(t)$, respectively.

By applying the coordinate transformations in Eqs. (33a,b) to Eq.(3), the following sets of $2m$ decoupled second-order *ODE*s is obtained:

$$\begin{aligned} &\ddot{\underset{\sim}{q}}_{j,k}(t) + 2\underset{\sim}{\xi}_{j,k}\, \underset{\sim}{\omega}_{j,k}\, \dot{\underset{\sim}{q}}_{j,k}(t) + \underset{\sim}{\omega}_{j,k}^2\, \underset{\sim}{q}_{j,k}(t) = \underset{\sim}{\boldsymbol{\phi}}_{j,k}^T \mathbf{f}(t); \\ &\ddot{\tilde{q}}_{j,k}(t) + 2\tilde{\xi}_{j,k}\, \tilde{\omega}_{j,k}\, \dot{\tilde{q}}_{j,k}(t) + \tilde{\omega}_{j,k}^2\, \tilde{q}_{j,k}(t) = \tilde{\boldsymbol{\phi}}_{j,k}^T \mathbf{f}(t), \quad (k = 1,2,\ldots,m) \end{aligned} \tag{34a,b}$$

with $\underset{\sim}{\omega}_{j,k}^2 \equiv \underset{\sim}{\lambda}_{j,k}$ and $\tilde{\omega}_{j,k}^2 \equiv \tilde{\lambda}_{j,k}$, while $\underset{\sim}{\xi}_{j,k} = (c_M + c_K\, \underset{\sim}{\omega}_{j,k}^2)/2\underset{\sim}{\omega}_{j,k}$ and $\tilde{\xi}_{j,k} = (c_M + c_K\, \tilde{\omega}_{j,k}{}^2)/2\tilde{\omega}_{j,k}$ are evaluated according to the Rayleigh condition (4). Introducing the modal state variable vectors $\underset{\sim}{\mathbf{y}}_{j,k}(t)$ and $\tilde{\mathbf{y}}_{j,k}(t)$, defined as:

$$\begin{aligned} \underset{\sim}{\mathbf{y}}_{j,k}(t) &\equiv \underset{\sim}{\mathbf{y}}_{j,k}(\underset{\sim}{\boldsymbol{\alpha}}_{\mathrm{C},j}, t) = \begin{bmatrix} \underset{\sim}{q}_{j,k}(t) \\ \dot{\underset{\sim}{q}}_{j,k}(t) \end{bmatrix}; \\ \tilde{\mathbf{y}}_{j,k}(t) &\equiv \tilde{\mathbf{y}}_{j,k}(\tilde{\boldsymbol{\alpha}}_{\mathrm{C},j}, t) = \begin{bmatrix} \tilde{q}_{j,k}(t) \\ \dot{\tilde{q}}_{j,k}(t) \end{bmatrix}. \end{aligned} \tag{35a,b}$$

Eqs.(34a,b) can be rewritten in terms of state variables, as follows:

$$\begin{aligned}\dot{\underset{\sim}{\mathbf{y}}}_{j,k}(t) &= \underset{\sim}{\mathbf{D}}_{j,k}\,\underset{\sim}{\mathbf{y}}_{j,k}(t) + \underset{\sim}{\mathbf{V}}_{j,k}\,\mathbf{f}(t);\\ \dot{\tilde{\mathbf{y}}}_{j,k}(t) &= \tilde{\mathbf{D}}_{j,k}\,\tilde{\mathbf{y}}_{j,k}(t) + \tilde{\mathbf{V}}_{j,k}\,\mathbf{f}(t)\end{aligned} \tag{36a,b}$$

where $\underset{\sim}{\mathbf{D}}_{j,k}$ and $\tilde{\mathbf{D}}_{j,k}$ are $2\times 2$ matrices, while $\underset{\sim}{\mathbf{V}}_{j,k}$ and $\tilde{\mathbf{V}}_{j,k}$ are $2\times n$ matrices defined respectively, as:

$$\begin{aligned}&\underset{\sim}{\mathbf{D}}_{j,k} = \begin{bmatrix} 0 & 1 \\ -\underset{\sim}{\omega}_{j,k}^2 & -2\underset{\sim}{\xi}_{j,k}\,\underset{\sim}{\omega}_{j,k}\end{bmatrix};\quad \tilde{\mathbf{D}}_{j,k} = \begin{bmatrix} 0 & 1 \\ -\tilde{\omega}_{j,k}^2 & -2\tilde{\xi}_{j,k}\,\tilde{\omega}_{j,k}\end{bmatrix};\\ &\underset{\sim}{\mathbf{V}}_{j,k} = \begin{bmatrix} \mathbf{0} \\ \underset{\sim}{\boldsymbol{\phi}}_{j,k}^T\end{bmatrix};\qquad\qquad \tilde{\mathbf{V}}_{j,k} = \begin{bmatrix} \mathbf{0} \\ \tilde{\boldsymbol{\phi}}_{j,k}^T\end{bmatrix}.\end{aligned} \tag{37a-d}$$

### 5.1 Bounds of free vibrations

According to Eqs.(12a,b), once the modal analysis is performed, the *LB* and *UB* of the free vibrations of the $j$-th displacement component $u_j^I(t)$, evaluated by solving the set of *ODE*s (36a,b) for $\mathbf{f}(t)=\mathbf{0}$, are given by (see Eqs.(12a,b)):

$$\begin{aligned}\underline{u}_j(t) &= \min\left\{\sum_{k=1}^{m}\underset{\sim}{\phi}_{j,jk}\underset{\sim}{q}_{j,k}(t),\quad \sum_{k=1}^{m}\tilde{\phi}_{j,jk}\tilde{q}_{j,k}(t)\right\};\\ \overline{u}_j(t) &= \max\left\{\sum_{k=1}^{m}\underset{\sim}{\phi}_{j,jk}\underset{\sim}{q}_{j,k}(t),\quad \sum_{k=1}^{m}\tilde{\phi}_{j,jk}\tilde{q}_{j,k}(t)\right\},\end{aligned} \tag{38a,b}$$

where $\underset{\sim}{q}_{j,k}(t)$ and $\tilde{q}_{j,k}(t)$ are the first elements of the following vectors, respectively:

$$\underset{\sim}{\mathbf{y}}_{j,k}(t) = \underset{\sim}{\boldsymbol{\Theta}}_{j,k}(t-t_0)\,\underset{\sim}{\mathbf{y}}_{j,k}(t_0);\quad \tilde{\mathbf{y}}_{j,k}(t) = \tilde{\boldsymbol{\Theta}}_{j,k}(t-t_0)\,\tilde{\mathbf{y}}_{j,k}(t_0) \tag{39a,b}$$

where $\underset{\sim}{\boldsymbol{\Theta}}_{j,k}(t)$ and $\tilde{\boldsymbol{\Theta}}_{j,k}(t)$ are the $2\times 2$ transition matrices given, respectively, as:

$$\underset{\sim}{\mathbf{\Theta}}_{j,k}(t)=\exp\left[t\ \underset{\sim}{\mathbf{D}}_{j,k}\right]=\begin{bmatrix}-\underset{\sim}{g}_{j,k}(t)\underset{\sim}{\omega}_{j,k}^2 & \dot{\underset{\sim}{g}}_{j,k}(t)\\ -\dot{\underset{\sim}{g}}_{j,k}(t)\underset{\sim}{\omega}_{j,k}^2 & \ddot{\underset{\sim}{g}}_{j,k}(t)\end{bmatrix};$$
$$\tilde{\mathbf{\Theta}}_{j,k}(t)=\exp\left[t\ \tilde{\mathbf{D}}_{j,k}\right]=\begin{bmatrix}-\tilde{g}_{j,k}(t)\tilde{\omega}_{j,k}^2 & \dot{\tilde{g}}_{j,k}(t)\\ -\dot{\tilde{g}}_{j,k}(t)\tilde{\omega}_{j,k}^2 & \ddot{\tilde{g}}_{j,k}(t)\end{bmatrix}. \tag{40a,b}$$

In the previous equations, $\underset{\sim}{g}_{j,k}(t)$ and $\tilde{g}_{j,k}(t)$ are two functions of time $t$, given, respectively, by:

$$\underset{\sim}{g}_{j,k}(t)=-\frac{1}{\underset{\sim}{\omega}_{j,k}^2}\exp(-\underset{\sim}{\xi}_{j,k}\underset{\sim}{\omega}_{j,k}t)\left[\cos\left(\underset{\sim}{\omega}_{j,k}t\sqrt{1-\underset{\sim}{\xi}_{j,k}^2}\right)+\frac{\underset{\sim}{\xi}_{j,k}}{\sqrt{1-\underset{\sim}{\xi}_{j,k}^2}}\operatorname{sen}\left(\underset{\sim}{\omega}_{j,k}t\sqrt{1-\underset{\sim}{\xi}_{j,k}^2}\right)\right];$$
$$\tilde{g}_{j,k}(t)=-\frac{1}{\tilde{\omega}_{j,k}^2}\exp(-\tilde{\xi}_{j,k}\tilde{\omega}_{j,k}t)\left[\cos\left(\tilde{\omega}_{j,k}t\sqrt{1-\tilde{\xi}_{j,k}^2}\right)+\frac{\tilde{\xi}_{j,k}}{\sqrt{1-\tilde{\xi}_{j,k}^2}}\operatorname{sen}\left(\tilde{\omega}_{j,k}t\sqrt{1-\tilde{\xi}_{j,k}^2}\right)\right]. \tag{41a,b}$$

### 5.2 Bounds of the time-history interval response

In order to evaluate the bounds of response time-history under an arbitrary deterministic dynamic excitation, the *ODE*s in Eq. (36a,b) need to be solved. As well known, the response time-history, in terms of state variables, of quiescent structural systems can be written in integral form as follows:

$$\underset{\sim}{\mathbf{y}}_{j,k}(t)=\int_0^t\underset{\sim}{\mathbf{\Theta}}_{j,k}\left(t-\tau\right)\underset{\sim}{\mathbf{V}}_{j,k}\,\mathbf{f}(\tau)\,\mathrm{d}\tau\ ;$$
$$\tilde{\mathbf{y}}_{j,k}(t)=\int_0^t\tilde{\mathbf{\Theta}}_{j,k}\left(t-\tau\right)\tilde{\mathbf{V}}_{j,k}\,\mathbf{f}(\tau)\,\mathrm{d}\tau \tag{42a,b}$$

where the matrices defined in Eqs.(37) and (40) appear. The solution of the integrals in Eqs. (42a,b) can be conveniently evaluated by a step-by-step numerical procedure (e.g. [27][28]). Specifically, subdividing the time interval of interest $0<t\le t_F$ into $N$ time steps $\Delta t=t_F/N$,

such that $t_s = s\Delta t$ ($s = 0,1,2,\ldots,N$), the following step-by step solutions of Eqs. (42a,b) are obtained:

$$\begin{aligned}
\underset{\sim}{\mathbf{y}}_{j,k}(t_{s+1}) &= \underset{\sim}{\boldsymbol{\Theta}}_{j,k}(\Delta t)\,\underset{\sim}{\mathbf{y}}_{j,k}(t_s) + \underset{\sim}{\boldsymbol{\gamma}}^{(0)}_{j,k}(\Delta t)\,\underset{\sim}{\mathbf{V}}_{j,k}\ \mathbf{f}(t_s) + \underset{\sim}{\boldsymbol{\gamma}}^{(1)}_{j,k}(\Delta t)\,\underset{\sim}{\mathbf{V}}_{j,k}\ \mathbf{f}(t_{s+1});\\
\tilde{\mathbf{y}}_{j,k}(t_{s+1}) &= \tilde{\boldsymbol{\Theta}}_{j,k}(\Delta t)\,\tilde{\mathbf{y}}_{j,k}(t_s) + \tilde{\boldsymbol{\gamma}}^{(0)}_{j,k}(\Delta t)\,\tilde{\mathbf{V}}_{j,k}\ \mathbf{f}(t_s) + \tilde{\boldsymbol{\gamma}}^{(1)}_{j,k}(\Delta t)\,\tilde{\mathbf{V}}_{j,k}\ \mathbf{f}(t_{s+1})
\end{aligned} \tag{43a,b}$$

where:

$$\begin{aligned}
&\underset{\sim}{\mathbf{L}}_{j,k}(\Delta t) = \left[\underset{\sim}{\boldsymbol{\Theta}}_{j,k}(\Delta t) - \mathbf{I}_2\right]\left(\underset{\sim}{\mathbf{D}}_{j,k}\right)^{-1}; \qquad && \tilde{\mathbf{L}}_{j,k}(\Delta t) = \left[\tilde{\boldsymbol{\Theta}}_{j,k}(\Delta t) - \mathbf{I}_2\right]\left(\tilde{\mathbf{D}}_{j,k}\right)^{-1};\\
&\underset{\sim}{\boldsymbol{\gamma}}^{(0)}_{j,k}(\Delta t) = \left[\underset{\sim}{\boldsymbol{\Theta}}_{j,k}(\Delta t) - \frac{1}{\Delta t}\underset{\sim}{\mathbf{L}}_{j,k}(\Delta t)\right]\left(\underset{\sim}{\mathbf{D}}_{j,k}\right)^{-1}; && \tilde{\boldsymbol{\gamma}}^{(0)}_{j,k}(\Delta t) = \left[\tilde{\boldsymbol{\Theta}}_{j,k}(\Delta t) - \frac{1}{\Delta t}\tilde{\mathbf{L}}_{j,k}(\Delta t)\right]\left(\tilde{\mathbf{D}}_{j,k}\right)^{-1};\\
&\underset{\sim}{\boldsymbol{\gamma}}^{(1)}_{j,k}(\Delta t) = \left[\frac{1}{\Delta t}\underset{\sim}{\mathbf{L}}_{j,k}(\Delta t) - \mathbf{I}_2\right]\left(\underset{\sim}{\mathbf{D}}_{j,k}\right)^{-1}; && \tilde{\boldsymbol{\gamma}}^{(1)}_{j,k}(\Delta t) = \left[\frac{1}{\Delta t}\tilde{\mathbf{L}}_{j,k}(\Delta t) - \mathbf{I}_{2m}\right]\left(\tilde{\mathbf{D}}_{j,k}\right)^{-1}.
\end{aligned} \tag{44a-f}$$

Finally, the *LB* and *UB*, $\underline{u}_j(t_{s+1})$ and $\overline{u}_j(t_{s+1})$, of the *j*-th displacement component can be obtained at each time instant $t_{s+1}$, according to Eqs.(12a,b), as follows:

$$\begin{aligned}
\underline{u}_j(t_{s+1}) &= \min\left\{\sum_{k=1}^{m}\underset{\sim}{\phi}_{j,jk}\underset{\sim}{q}_{j,k}(t_{s+1}),\ \sum_{k=1}^{m}\tilde{\phi}_{j,jk}\tilde{q}_{j,k}(t_{s+1})\right\};\\
\overline{u}_j(t_{s+1}) &= \max\left\{\sum_{k=1}^{m}\underset{\sim}{\phi}_{j,jk}\underset{\sim}{q}_{j,k}(t_{s+1}),\ \sum_{k=1}^{m}\tilde{\phi}_{j,jk}\tilde{q}_{j,k}(t_{s+1})\right\}.
\end{aligned} \tag{45a,b}$$

The proposed method for the dynamic analysis of structures with uncertain-but-bounded parameters under arbitrary dynamic excitation is summarized in the following flow-chart:

- Input data: geometry, boundary and loading conditions, material properties of the nominal structure; uncertain parameters $d_i^I = d_{0,i}(1+\alpha_i^I)$, ($i = 1,2,\ldots,r$)
- Define the nominal matrices $\mathbf{M}_0$, $\mathbf{K}_0$, and $\mathbf{C}_0$
- Solve the nominal eigenproblem in Eq. (27)
- Solve Eq.(28) to evaluate the nominal dynamic response $\mathbf{u}_0(t)$ by using Eq. (26)

- Evaluate the matrices $\mathbf{K}_\ell$, $(\ell = 1,2,\ldots,r)$, in Eq. (24)
- Evaluate the *pseudo-static sensitivity* vectors $\mathbf{s}_{\mathbf{u},\ell}(t)$, $(\ell = 1,2,\ldots,r)$
- Define the vectors $\underset{\sim}{\boldsymbol{\alpha}}_{\mathrm{C},j}$ and $\tilde{\boldsymbol{\alpha}}_{\mathrm{C},j}$ (Eqs.31(a,b)) collecting the most common combinations of the endpoints of the uncertain parameters to be used for evaluating $\underline{u}_j(t)$ and $\overline{u}_j(t)$, respectively
- Solve two deterministic eigenproblems (Eqs. (32a,b)) associated to $\underset{\sim}{\boldsymbol{\alpha}}_{\mathrm{C},j}$ and $\tilde{\boldsymbol{\alpha}}_{\mathrm{C},j}$
- Perform two parallel step-by-step numerical integrations to evaluate the modal responses associated to $\underset{\sim}{\boldsymbol{\alpha}}_{\mathrm{C},j}$ and $\tilde{\boldsymbol{\alpha}}_{\mathrm{C},j}$ (see Eqs. (43a,b))
- Evaluate the bounds of the *j*-th displacement component using Eqs. (45a,b)

## 6 NUMERICAL APPLICATIONS

To validate the proposed method, three numerical applications concerning quite different types of structural systems are presented: a 3D truss structure, a grid structure and a shell corner. In all the examples, Young's modulus of the material is assumed to be uncertain. The accuracy of the proposed procedure is assessed by comparison with the exact bounds of the selected dynamic response quantities of interest provided by the *vertex method* [25]. The latter is a combinatorial procedure which requires to perform as many deterministic dynamic analyses as are the possible combinations of the bounds of the $r$ uncertain-but-bounded parameters, say $2^r$, and then seek, at each time instant, the minimum and maximum among the computed responses. Appropriate comparisons with the bounds obtained considering the *trivial* combinations of the endpoints of the uncertain parameters and by applying the *IPM* are also presented. FE models of the analyzed structures are built by using the commercial software ABAQUS which is also exploited to perform the deterministic dynamic analyses requested both by the proposed procedure and the *vertex method*.

### 6.1 3D truss structure with uncertain Young's modulus under impulsive load

As first application, the 3D 26-bar truss structure with 18 DOFs depicted in Figure 1 is considered. The following geometrical and mechanical properties are assumed: nominal cross-sectional area of the bars $A_0 = A_{0,i} = 4.27 \times 10^{-4}$ m$^2$ , nominal Young's moduli $E_0 = E_{0,i} = 2.1 \times 10^8$ kN/m$^2$ , ( $i = 1,2,\ldots,26$ ), nominal mass $m_{0,j} = m_0 = 1000$ kg , ( $j = 1,2,\ldots,6$ ), lumped at each node. The Rayleigh damping constants $c_M$ and $c_K$ in Eq.(4) have been taken as $c_M = 3.28904$ s$^{-1}$ and $c_K = 0.00076$ s , respectively, in such a way that the modal damping ratio for the first and second modes of the nominal structure is $\xi_0 = 0.05$ . The truss is subjected to an impulsive load, $f(t) = f_0 \delta(t) = 1000\,\delta(t)$ N , as shown in Figure 1. Young's moduli of $r = 13$ bars are modeled as interval variables, $E_i^I = E_0(1 + \Delta\alpha \hat{e}_i^I)$ , ( $i = 1,2,\ldots,13$ ), (see bar numbering in Figure 1), with the same deviation amplitude $\Delta\alpha < 1$. The interval displacement of node A in the load direction, $u_{\mathrm{A}y}^I(t)$ , is selected as response quantity of interest.

According to Eqs. (42a,b), the two dynamic responses of the truss structure under the impulsive load, pertaining to the most common combinations of the bounds of the uncertain parameters, $\underset{\sim}{\boldsymbol{\alpha}}_{\mathrm{C},j}$ and $\tilde{\boldsymbol{\alpha}}_{\mathrm{C},j}$ , can be evaluated in closed-form as:

$$\underset{\sim}{\mathbf{y}}_{j,k}(t) = \underset{\sim}{\boldsymbol{\Theta}}_{j,k}(t)\,\underset{\sim}{\mathbf{v}}_{j,k}\,; \quad \tilde{\mathbf{y}}_{j,k}(t) = \tilde{\boldsymbol{\Theta}}_{j,k}(t)\,\tilde{\mathbf{v}}_{j,k} \tag{46a,b}$$

where

$$\underset{\sim}{\mathbf{v}}_{j,k} = \begin{bmatrix} 0 \\ \underset{\sim}{\boldsymbol{\phi}}_{j,k}^T \end{bmatrix} f_0; \qquad \tilde{\mathbf{v}}_{j,k} = \begin{bmatrix} 0 \\ \tilde{\boldsymbol{\phi}}_{j,k}^T \end{bmatrix} f_0. \tag{47a-d}$$

Figures 2 and 3 display the time-histories of the *LB* and *UB* of the interval nodal displacement $u_{\mathrm{A}y}^I(t)$ for two deviation amplitudes of the uncertain-but-bounded parameters, say

$\Delta\alpha = 0.1$ and $\Delta\alpha = 0.2$, respectively. The proposed bounds are compared with the ones obtained by applying the *IPM* as well as with the exact bounds provided by the *vertex method*, which requires $2^{13}$ deterministic dynamic analyses. By inspection of these figures, it can be observed that the proposed method is more accurate than the *IPM*. In particular, as larger degrees of uncertainty are considered, say $\Delta\alpha = 0.2$ (see Figure 3), the accuracy of the *IPM* rapidily worsens, while the proposed bounds of the dynamic response are still very close to the exact ones. Furthermore, it is worth observing that the *IPM* generally overestimates the interval response.

### 6.2 Grid structure with uncertain Young's modulus under impulsive load

The second application concerns the grid structure shown in Figure 4 which represents part of the roof of an existing building located in Italy. The grid structure is made of concrete with the following mechanical properties: nominal Young's modulus $E_0 = 3.15\times10^7\ \text{kN/m}^2$, Poisson's ratio $\nu = 0.2$, unit weight $\gamma = 25\,\text{kN/m}^3$. A consistent mass matrix is considered. The FE model of the grid structure consists of 142 frame FEs with rectangular cross-section having width $0.80$ m and thickness $0.20$ m. The total number of DOFs is $n = 474$. The Rayleigh damping constants $c_M$ and $c_K$ in Eq.(4) have been taken as $c_M = 2.89598\ \text{s}^{-1}$ and $c_K = 0.00074$ s, respectively, in such a way that the modal damping ratio for the first and third modes of the nominal structure is $\xi_0 = 0.05$. The grid structure is subjected to an impulsive load, $f(t) = f_0\,\delta(t) = 20\,\delta(t)\,\text{kN}$, applied to the central node A, as shown in Figure 4. Young's moduli of $r = 9$ elements are modeled as interval variables, $E_i^I = E_0(1+\Delta\alpha\hat{e}_i^I)$, ($i = 1,2,\ldots,r = 9$), (see element numbering in Figure 4), with the same deviation amplitude $\Delta\alpha < 1$. The selected response quantities of interest are the interval displacement of node A in the load direction, $u_{\text{Az}}^I(t)$, the interval rotations of node A, $\varphi_{\text{Ax}}^I(t)$ and $\varphi_{\text{Ay}}^I(t)$, around the $x$-

and $y$ -axes, respectively (see Figure 4). Also in this case, the two dynamic responses pertaining to the most common combinations of the bounds of the uncertain parameters can be evaluated in closed-form (see Eqs. (46a,b)).

Figures 5 and 6 show the time-histories of the *LB* and *UB*, respectively, of the interval displacement, $u_{\mathrm{Az}}^{I}(t)$, and rotations of node A, $\varphi_{\mathrm{Ax}}^{I}(t)$ and $\varphi_{\mathrm{Ay}}^{I}(t)$, for a deviation amplitude of the uncertain parameters $\Delta\alpha = 0.1$. The proposed estimates are compared with the ones provided by the *IPM* and *vertex method*. Similar comparisons are shown in Figures 7 and 8 for a larger degree of uncertainty, say $\Delta\alpha = 0.2$. It can be observed that both the proposed method and the *IPM* yield accurate estimates of the bounds of the interval displacement $u_{\mathrm{Az}}^{I}(t)$. Conversely, the proposed bounds of the interval rotations of node A, $\varphi_{\mathrm{Ax}}^{I}(t)$ and $\varphi_{\mathrm{Ay}}^{I}(t)$, are much more accurate than the ones provided by the *IPM*, especially when larger fluctuations of the uncertain parameters are considered. It is worth mentioning that, for real-size systems, like the grid structure herein examined, the *IPM* is much more expensive and involved than the proposed method.

To further assess the effectiveness of the presented procedure, in Figures 9 and 10 the proposed *LB* and *UB* of the selected response quantities of interest are contrasted with the exact bounds and the ones obtained considering the *trivial* combinations of the endpoints of the uncertain parameters, for $\Delta\alpha = 0.2$. By inspection of Figures 9a and 10a, it is inferred that the most common combinations yielding the bounds of the interval displacement $u_{\mathrm{Az}}^{I}(t)$ according to the proposed *pseudo-static sensitivity* analysis actually are the same as the *trivial* ones. Specifically, the proposed *LB* and *UB* of $u_{\mathrm{Az}}^{I}(t)$ are obtained setting, at each time instant, all the uncertain parameters equal to their *LB* and *UB*, respectively. Conversely, the most common combinations detected by the proposed *pseudo-static sensitivity* analysis for the evaluation of the bounds of the rotations of node A, $\varphi_{\mathrm{Ax}}^{I}(t)$ and $\varphi_{\mathrm{Ay}}^{I}(t)$, are different from the *trivial*

ones. Indeed, Figures 9b,c and 10b,c show that the proposed estimates of the bounds of $\varphi^I_{Ax}(t)$ and $\varphi^I_{Ay}(t)$ are much more accurate than the ones pertaining to the *trivial* combinations.

### 6.3 Shell corner with uncertain Young's modulus under seismic excitation

As last application, a shell corner subjected to the component of ground motion acceleration recorded at El Centro along the $x-$direction is considered (see Figure 11). The following geometrical and mechanical properties are assumed: nominal Young's modulus $E_0 = 3.15\times10^7\,\text{kN/m}^2$, Poisson's ratio $\nu = 0.2$, unit weight $\gamma = 25\,\text{kN/m}^3$, thickness $s = 0.25\,\text{m}$. The FE model built in ABAQUS consists of 198 shell FEs with 6 DOFs per node (S8R), so that the total number of DOFs is $n = 3960$. A consistent mass matrix is considered. The Rayleigh damping constants $c_M$ and $c_K$ in Eq.(4) have been taken as $c_M = 1.83015\,\text{s}^{-1}$ and $c_K = 0.00135\,\text{s}$, respectively, in such a way that the modal damping ratio for the first and fourth modes of the nominal structure is $\xi_0 = 0.05$. Young's moduli of the $r = 6$ sub-domains highlighted in Figure 11 are modeled as independent interval variables, $E^I_i = E_0(1+\Delta\alpha\hat{e}^I_i)$, ($i = 1,2,\ldots,r = 6$), with the same deviation amplitude $\Delta\alpha < 1$. The interval displacement of node A in the $x$-direction, $u^I_{Ax}(t)$, is selected as response quantity of interest.

In Figure 12, the time-histories of the *LB* and *UB* of the interval displacement $u^I_{Ax}(t)$ for $\Delta\alpha = 0.1$ and $\Delta\alpha = 0.2$, respectively, are plotted. For the sake of clarity, the *LB* (negative values) and *UB* (positive values) are reported in the same plot. The proposed estimates are contrasted to the bounds provided by the *IPM* and *vertex method*. It can be observed that the *IPM* highly overestimates the region of the interval response even for $\Delta\alpha = 0.1$. Conversely, the proposed bounds of the interval displacement $u^I_{Ax}(t)$ are very close to the exact ones even when larger degrees of uncertainty are considered, say $\Delta\alpha = 0.2$.

Finally, in Figure 13 the proposed time-histories of the *LB* and *UB* of the interval displacement $u_{Ax}^I(t)$ are compared with the exact bounds and the ones obtained considering the *trivial* combinations of the endpoints of the uncertain parameters, for $\Delta\alpha = 0.2$. It can be seen that the most common combinations provided by the proposed *pseudo-static sensitivity* analysis are different from the *trivial* ones and provide more accurate estimates of the bounds of the response. Specifically, the proposed *LB* of the interval displacement $u_{Ax}^I(t)$ at each time instant is evaluated considering the following "Commonest" combinations $E_1 = \underline{E}_1,\ E_i = \overline{E}_i, i = 2,\ldots,6$; while the proposed time-history of the *UB* is obtained assuming $E_1 = \overline{E}_1,\ E_i = \underline{E}_i, i = 2,\ldots,6$. It is worth noting that, though the "Commonest" combinations differ from the *trivial* ones only for the value assumed by $E_1 \in E_1^I$, the corresponding bounds of the displacement $u_{Ax}^I(t)$ are closer to the exact ones.

## 7 CONCLUSIONS

The challenging task of evaluating the bounds of the response of linear-elastic structures with uncertain-but-bounded properties subjected to deterministic dynamic excitations has been addressed. In the framework of the classical modal analysis, a novel method has been developed as an appropriate extension of sensitivity-based procedures successfully applied in literature to predict the range of the interval structural response under static loads.

The proposed method basically requires to perform two parallel deterministic modal analyses corresponding to the values of the uncertain parameters selected by a *pseudo-static sensitivity* analysis and then seek, at each time instant, the minimum and maximum among the computed responses. The following main steps are required: *i*) a preliminary *pseudo-static sensitivity* analysis to define the most common combinations of the endpoints of the interval parameters to be used for estimating the *lower bound* and *upper bound* of the response over

the whole time-history; *ii*) two parallel modal analyses which require the solutions of two generalized eigenproblems and the step-by-step integration of two deterministic equations of motion in the modal sub-space corresponding to the most common combinations defined in the previous step; *iii*) the evaluation of the bounds of the response time-history as the minimum and maximum among the responses provided by the two parallel modal analyses at each time step.

Numerical results, focusing on the comparison of the proposed method with the *Interval Perturbation Method* (*IPM*) and the classical combinatorial procedure, have been presented.

The main advantages of the presented method may be summarized as follows: *i*) unlike the *IPM*, the proposed procedure provides very accurate estimates of the bounds of the dynamic response even in the presence of relatively large degrees of uncertainty; *ii*) the computational effort is much lower than the one requested both by the *IPM* and classical combinatorial procedure, especially for large-size structures with many uncertain parameters; *iii*) the non-intrusive nature of the main body of the numerical procedure, consisting of two deterministic modal analyses, allows the integration into standard finite element codes.

**ACKNOWLEDGMENT**

The support to this research by the PRIN2015, project No 2015TTJN95 entitled "Identification and monitoring of complex structural systems", is gratefully acknowledged.

**REFERENCES**

[1] R. W. Clough, J. Penzien, Dynamics of Structures, McGraw-Hill. New York, Second Edition, 1993.

[2] D. Moens, D. Vandepitte, A Survey of Non-Probabilistic Uncertainty Treatment in Finite Element Analysis. Comput. Methods Appl. Mech. Eng. 194 (2005) 1527-1555.

[3] Y. Ben-Haim, I. Elishakoff, Convex Models of Uncertainty in Applied Mechanics, Elsevier Science Publishers, Amsterdam, 1990.

[4] I. Elishakoff, M. Ohsaki, Optimization and Anti-Optimization of Structures under Uncertainties, Imperial College Press, London, 2010.

[5] R.E. Moore, Interval Analysis, Prentice-Hall, Englewood Cliffs, 1966.

[6] R.E. Moore, R.B. Kearfott, M.J. Cloud, Introduction to Interval Analysis, SIAM, Philadelphia, 2009.

[7] Z.P. Qiu and X.J. Wang, Vertex solution theorem for the upper and lower bounds on the dynamic response of structures with uncertain-but-bounded parameters, Acta Mech. Sinica 25 (2009) 367-379.

[8] A.D. Dimarogonas, Interval Analysis of Vibrating Systems, J. Sound Vib. 183 (1995) 739-749.

[9] J. Wu, Y. Zhang, L.Chen, Z. Luo, A Chebyshev interval method for nonlinear dynamic systems under uncertainty, Appl. Math. Model. 37 (2013) 4578-4591.

[10] S.H. Chen, H.D. Lian, X.W. Yang, Dynamic response analysis for structures with interval parameters, Struct. Eng. Mech. 13 (2002) 299-312.

[11] Z.P. Qiu, X.J. Wang, Comparison of dynamic response of structures with uncertain-but-bounded parameters using non probabilistic interval analysis method and probabilistic approach, Int. J. Solids Struct. 40 (2003) 5423-5439.

[12] Z.P. Qiu, X.J. Wang, Parameter perturbation method for dynamic responses of structures with uncertain-but-bounded parameters based on interval analysis, Int. J. Solids Struct. 42 (2005) 4958-4970.

[13] Z.P. Qiu, L.Ma, X.Wang, Non-probabilistic interval analysis method for dynamic response analysis of nonlinear systems with uncertainty, J. Sound Vib. 319 (2009) 531–540.

[14] Y. Xia, Z.P. Qiu, M.I. Friswell, The time response of the structure with bounded parameters and interval initial conditions, J. Sound Vib. 329 (2010) 353–365.

[15] G. Muscolino, A. Sofi, Response statistics of linear structures with uncertain-but-bounded parameters under Gaussian stochastic input, Int. J. Struct. Stab. Dy. 11 (2011) 775-804.

[16] W. Gao, N. Zhang, J. Ma, X.B. Wang, Interval dynamic response analysis of structures with interval parameters, Pr. Inst. Mech. Eng., Part C: J. Mech. Eng. Sci. 222 (2008) 377-385.

[17] M.V. Rama Rao, A. Pownuk, S. Vandewalle, D. Moens, Transient response of structures with uncertain structural parameters, Struct. Saf. 32 ( 2010) 449-460.

[18] Y.W. Yang, Z.H. Cai, Y. Liu, Interval analysis of dynamic response of structures using Laplace transform, Probab. Eng. Mech. 29 (2012) 32-39.

[19] B. Xia, D. Yu, Interval analysis of acoustic field with uncertain-but-bounded parameters, Comp. Struct. 112 (2012) 235-244.

[20] B. Xia, D. Yu, Modified sub-interval perturbation finite element method for 2D acoustic field prediction with large uncertain-but-bounded parameters, J. Sound Vib. 331 (2012) 3774-3790.

[21] B. Xia, D. Yu, Modified interval perturbation finite element method for a structural-acoustic system with interval parameters, J. Appl. Mech. (ASME) 80 (2013) 041027.1–041027.8.

[22] B. Xia, Y. Qin, D. Yu, C. Jiang, Dynamic response analysis of structure under time-variant interval process model, J. Sound Vib. 381 (2016) 121-138.

[23] A. Pownuk, Efficient method of solution of large scale engineering problems with interval parameters. In: Muhanna, RL, Mullen RL (eds), Proc. NSF Workshop on Reliable Engineering Computing, September 15–17, 2004, Savannah, Georgia, USA (2004) 305–316.

[24] A. Sofi, E. Romeo, A novel Interval Finite Element Method based on the improved interval analysis, Comput. Methods Appl. Mech. Eng. 311 (2016) 671 – 697.

[25] W. Dong, H. Shah Vertex method for computing functions of fuzzy variables, Fuzzy Sets Syst. 24 (1987) 65 – 78.

[26] G. Muscolino, A. Sofi, Stochastic response of structures with uncertain-but-bounded parameters via improved interval analysis, Probab. Eng. Mech. 28 (2012) 152-163.

[27] G. Borino, G. Muscolino, Mode-superposition methods in dynamic analysis of classically and non-classically damped linear systems, Earthquake Eng. Struct. Dy. 14 (1986) 705-717.

[28] G. Muscolino, Dynamically Modified Linear Structures: Deterministic and Stochastic Response, J. Eng. Mech. (ASCE) 122 (1996) 1044-1051.

[29] Z.P. Qiu, I. Elishakoff, J.H. Jr. Starnes, The bound set of possible eigenvalues of structures with uncertain but non-random parameters, Chaos, Solitons Fract. 7 (1996) 1854-1857.

[30] Z.P. Qiu, X.J. Wang, M.I. Friswell, Eigenvalue bounds of structures with uncertain-but-bounded parameters, J. Sound Vib. 282 (2005) 297–312.

[31] M. Modares, R.L. Mullen, R.L. Muhanna, Natural frequencies of a structure with bounded uncertainty, J. Eng. Mech. (ASCE), 132 (2006) 1363-1371.

[32] A. Sofi, G. Muscolino, I. Elishakoff. Natural frequencies of a structure with interval parameters, J. Sound Vib. 347 (2015) 79-95.

[33] D. Moens, D. Vandepitte, Interval sensitivity theory and its application to frequency response envelope analysis of uncertain structures, Comput. Methods Appl. Mech. Eng. 196 (2007) 2486-2496.

## Figure captions

**Figure 1.** 3D 26-bar truss structure with uncertain Young's moduli of $r = 13$ bars subjected to an impulsive load.

**Figure 2.** Time-histories of the a) *LB* and b) *UB* of the interval nodal displacement $u_{\mathrm{A}y}^{I}(t)$ of the 3D truss provided by the proposed method, *IPM* and *vertex method*, for a deviation amplitude of the uncertain parameters $\Delta\alpha = 0.1$.

**Figure 3.** Time-histories of the a) *LB* and b) *UB* of the interval nodal displacement $u_{\mathrm{A}y}^{I}(t)$ of the 3D truss provided by the proposed method, *IPM* and *vertex method*, for a deviation amplitude of the uncertain parameters $\Delta\alpha = 0.2$.

**Figure 4.** Grid structure with uncertain Young's moduli of $r = 9$ elements subjected to an impulsive load: a) 3D model; b) planar view.

**Figure 5.** Time-histories of the *LB* of the interval a) displacement $u_{\mathrm{A}z}^{I}(t)$ and rotations b) $\varphi_{\mathrm{A}x}^{I}(t)$, c) $\varphi_{\mathrm{A}y}^{I}(t)$ of node *A* of the grid structure provided by the proposed method, *IPM* and *vertex method*, for a deviation amplitude of the uncertain parameters $\Delta\alpha = 0.1$.

**Figure 6.** Time-histories of the *UB* of the interval a) displacement $u_{\mathrm{A}z}^{I}(t)$ and rotations b) $\varphi_{\mathrm{A}x}^{I}(t)$, c) $\varphi_{\mathrm{A}y}^{I}(t)$ of node *A* of the grid structure provided by the proposed method, *IPM* and *vertex method*, for a deviation amplitude of the uncertain parameters $\Delta\alpha = 0.1$.

**Figure 7.** Time-histories of the *LB* of the interval a) displacement $u_{\mathrm{A}z}^{I}(t)$ and rotations b) $\varphi_{\mathrm{A}x}^{I}(t)$, c) $\varphi_{\mathrm{A}y}^{I}(t)$ of node *A* of the grid structure provided by the proposed method, *IPM* and *vertex method*, for a deviation amplitude of the uncertain parameters $\Delta\alpha = 0.2$.

**Figure 8.** Time-histories of the *UB* of the interval a) displacement $u_{\mathrm{A}z}^{I}(t)$ and rotations b) $\varphi_{\mathrm{A}x}^{I}(t)$, c) $\varphi_{\mathrm{A}y}^{I}(t)$ of node *A* of the grid structure provided by the proposed method, *IPM* and *vertex method* for a deviation amplitude of the uncertain parameters $\Delta\alpha = 0.2$.

**Figure 9.** Time-histories of the *LB* of the interval a) displacement $u_{\mathrm{A}z}^{I}(t)$ and rotations b) $\varphi_{\mathrm{A}x}^{I}(t)$, c) $\varphi_{\mathrm{A}y}^{I}(t)$ of node *A* of the grid structure obtained applying the proposed method, the *vertex method* and considering the *trivial* combinations of the endpoints of the uncertain parameters for $\Delta\alpha = 0.2$.

**Figure 10.** Time-histories of the *UB* of the interval a) displacement $u_{\mathrm{A}z}^{I}(t)$ and rotations b) $\varphi_{\mathrm{A}x}^{I}(t)$, c) $\varphi_{\mathrm{A}y}^{I}(t)$ of node *A* of the grid structure obtained applying the proposed method, the *vertex method* and considering the *trivial* combinations of the endpoints of the uncertain parameters for $\Delta\alpha = 0.2$.

**Figure 11.** Shell corner with uncertain Young's moduli of $r = 6$ sub-domains under El Centro ground motion acceleration along the $x-$direction.

**Figure 12.** Time-histories of the *LB* and *UB* of the interval displacement $u_{\mathrm{A}x}^{I}(t)$ of the shell corner provided by the proposed method, *IPM* and *vertex method*, for a deviation amplitude of the uncertain parameters a) $\Delta\alpha = 0.1$ and b) $\Delta\alpha = 0.2$.

**Figure 13.** Time-histories of the *LB* and *UB* of the interval displacement $u_{\mathrm{A}x}^{I}(t)$ of the shell corner obtained applying the proposed method, the *vertex method* and considering the *trivial* combinations of the endpoints of the uncertain parameters, for $\Delta\alpha = 0.2$.

**Figure 1**

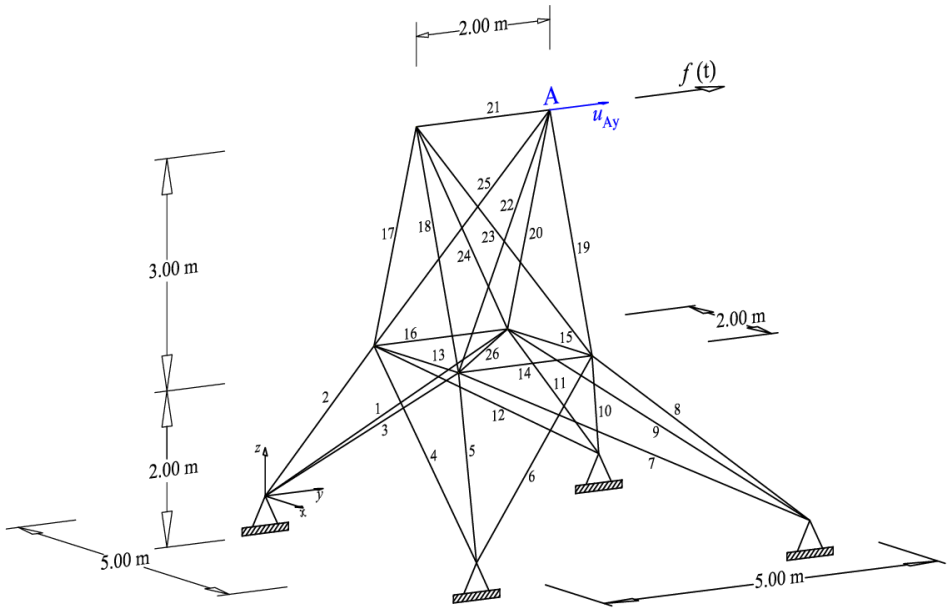


**Figure 1.** 3D 26-bar truss structure with uncertain Young's moduli of $r = 13$ bars subjected to an impulsive load.

**Figure 2**

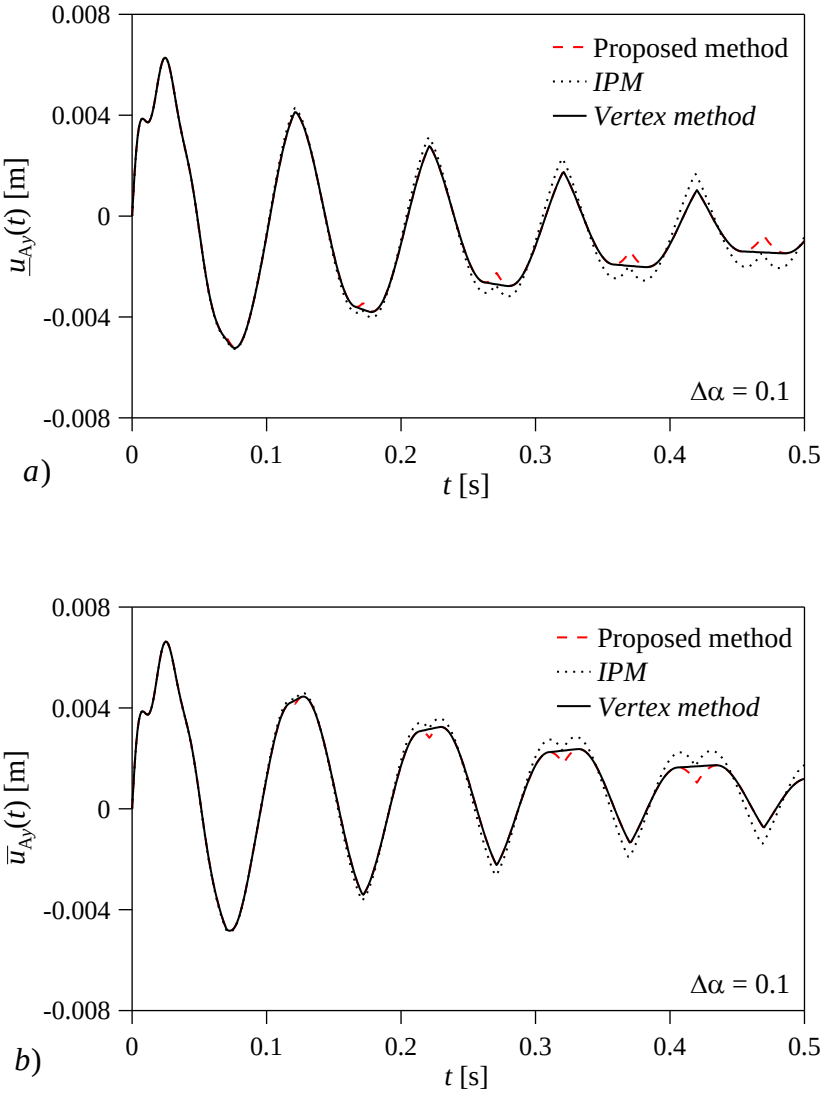


**Figure 2.** Time-histories of the a) *LB* and b) *UB* of the interval nodal displacement $u_{Ay}^{I}(t)$ of the 3D truss provided by the proposed method, *IPM* and *vertex method*, for a deviation amplitude of the uncertain parameters $\Delta\alpha = 0.1$.

**Figure 3**

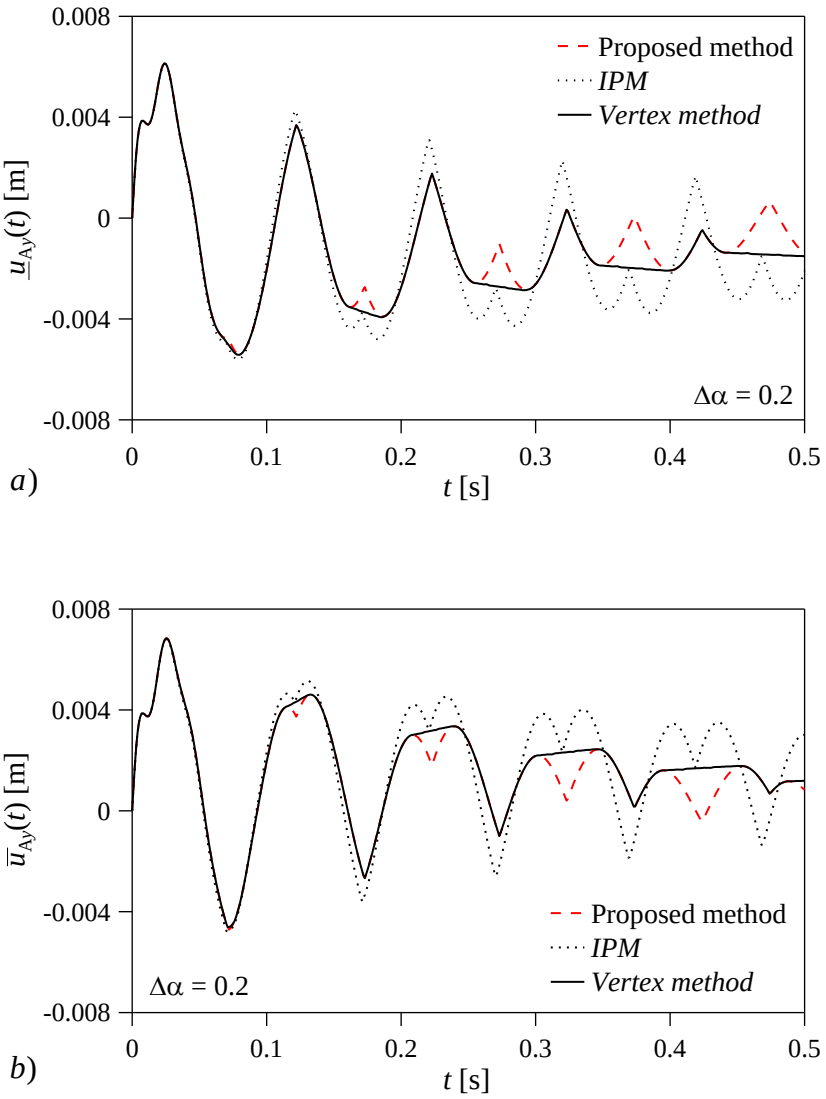


**Figure 3.** Time-histories of the a) *LB* and b) *UB* of the interval nodal displacement $u^I_{Ay}(t)$ of the 3D truss provided by the proposed method, *IPM* and *vertex method*, for a deviation amplitude of the uncertain parameters $\Delta\alpha = 0.2$.

**Figure 4**

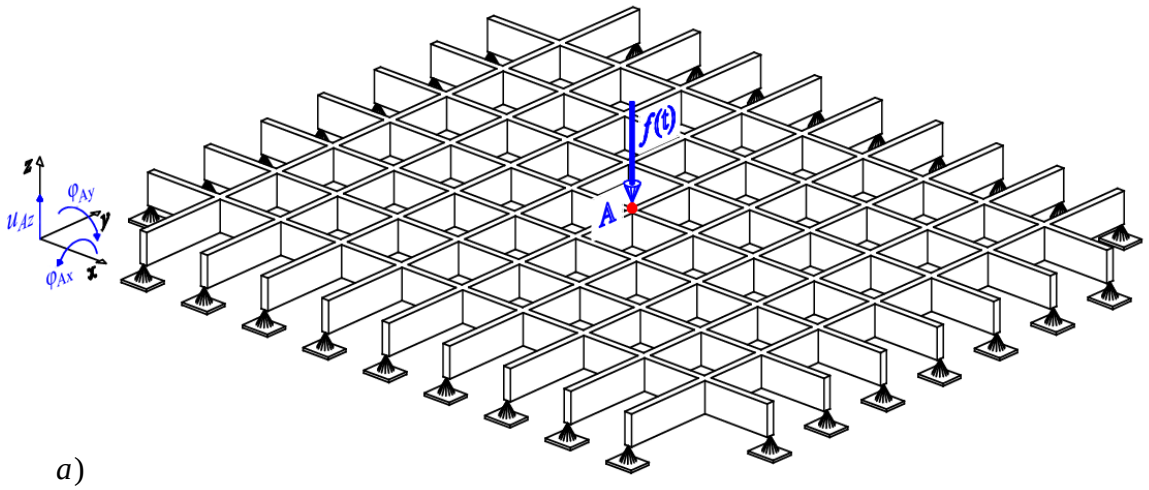


*a*)

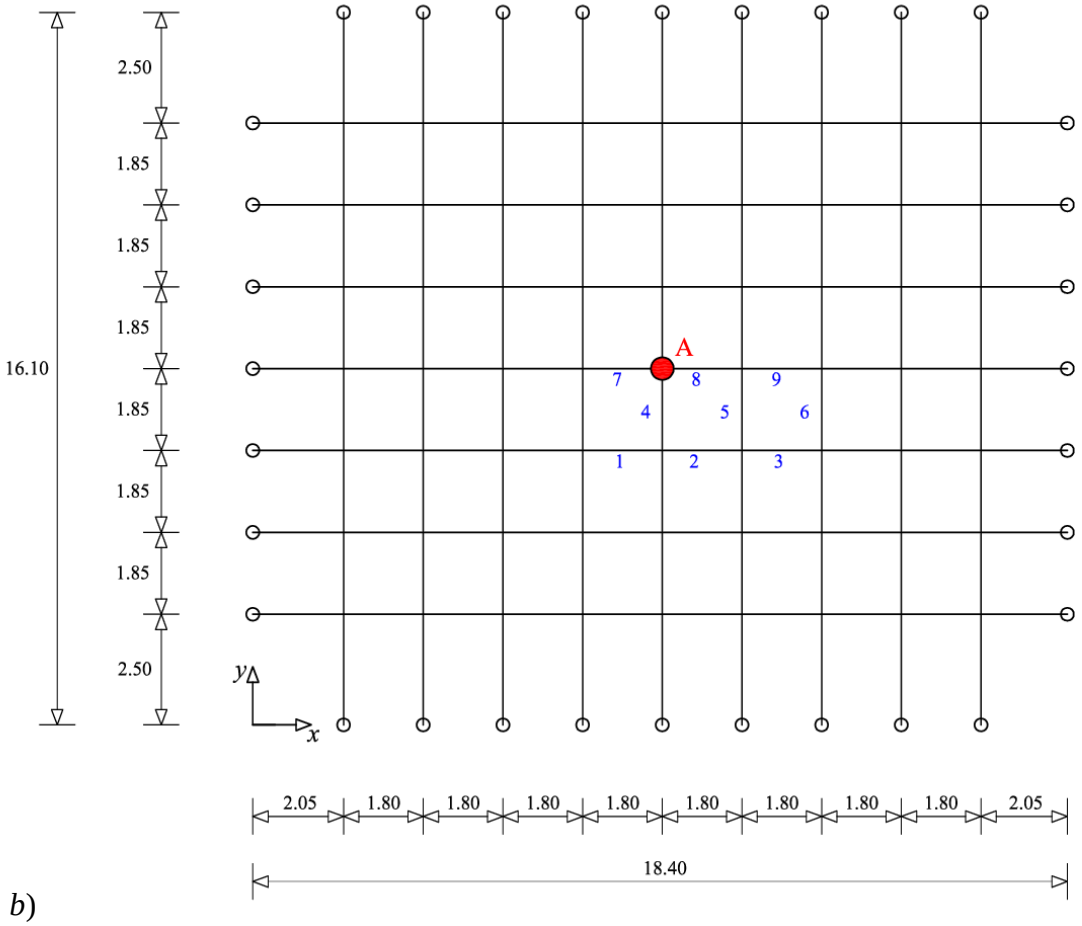


*b*)

**Figure 4.** Grid structure with uncertain Young's moduli of $r = 9$ elements subjected to an impulsive load: a) 3D model; b) planar view.

**Figure 5**

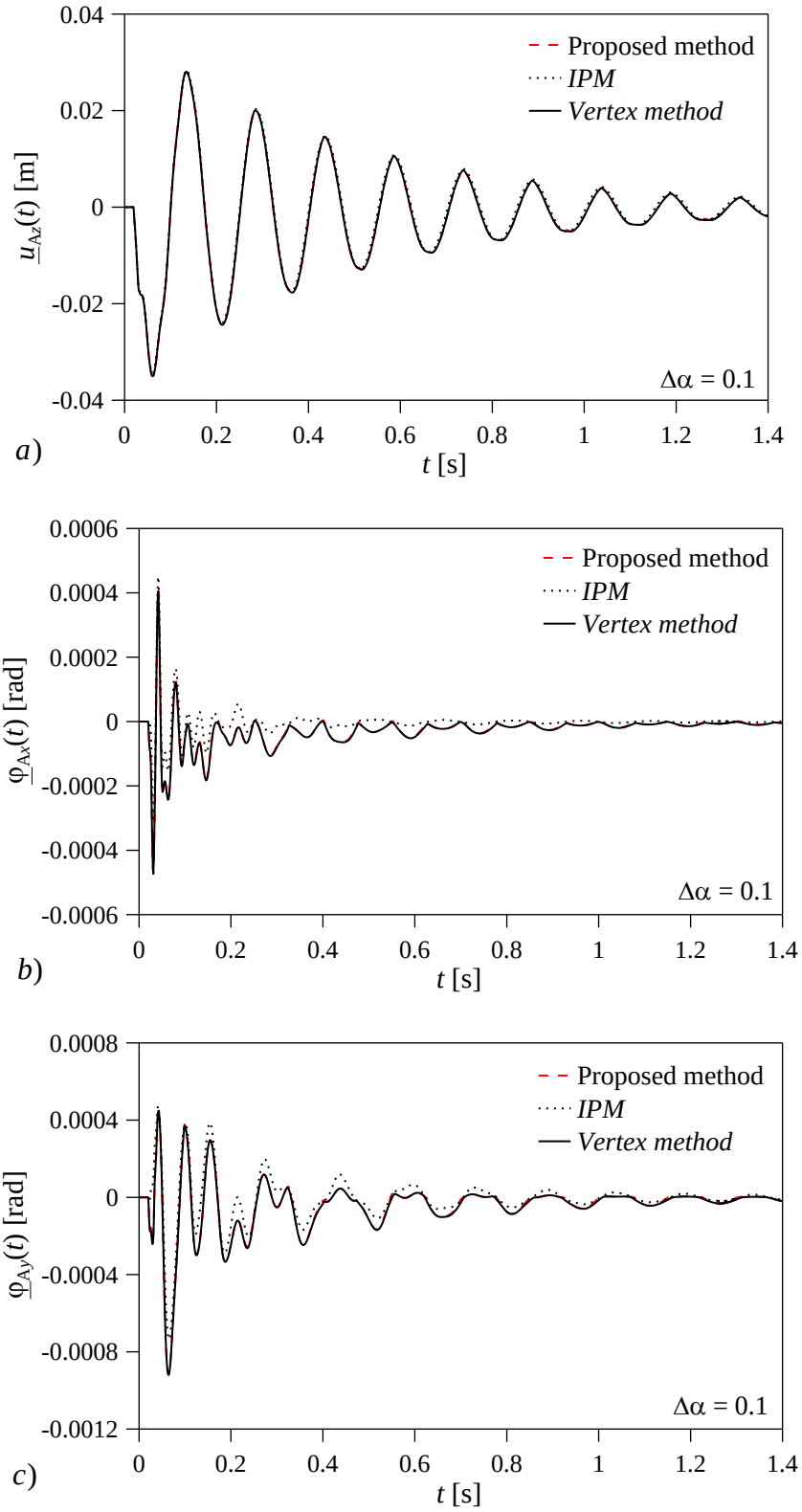


**Figure 5.** Time-histories of the *LB* of the interval a) displacement $u^I_{Az}(t)$ and rotations b) $\varphi^I_{Ax}(t)$, c) $\varphi^I_{Ay}(t)$ of node *A* of the grid structure provided by the proposed method, *IPM* and *vertex method*, for a deviation amplitude of the uncertain parameters $\Delta\alpha = 0.1$.

**Figure 6**

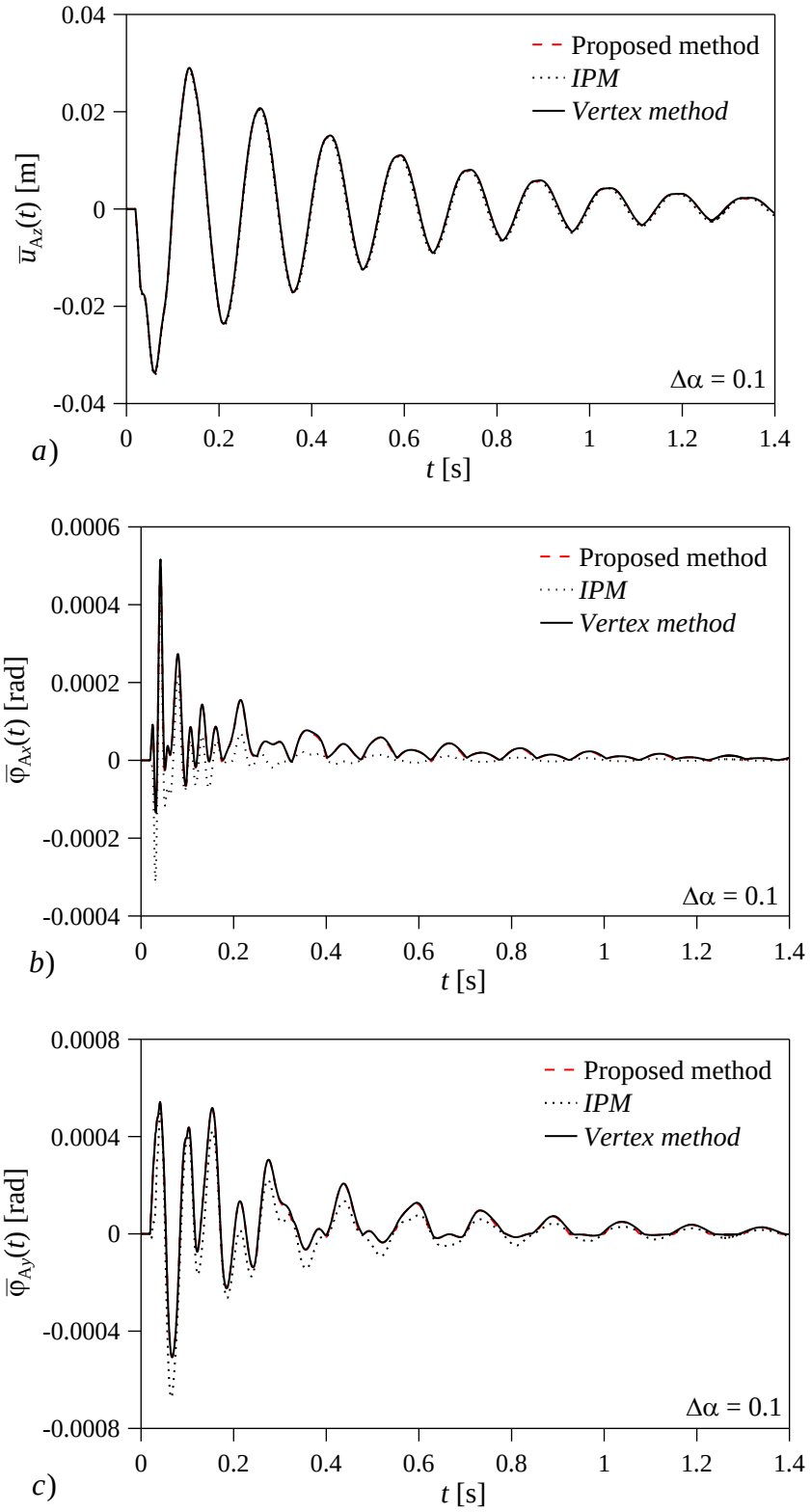


**Figure 6.** Time-histories of the *UB* of the interval a) displacement $u^I_{Az}(t)$ and rotations b) $\varphi^I_{Ax}(t)$, c) $\varphi^I_{Ay}(t)$ of node *A* of the grid structure provided by the proposed method, *IPM* and *vertex method*, for a deviation amplitude of the uncertain parameters $\Delta\alpha = 0.1$.

**Figure 7**

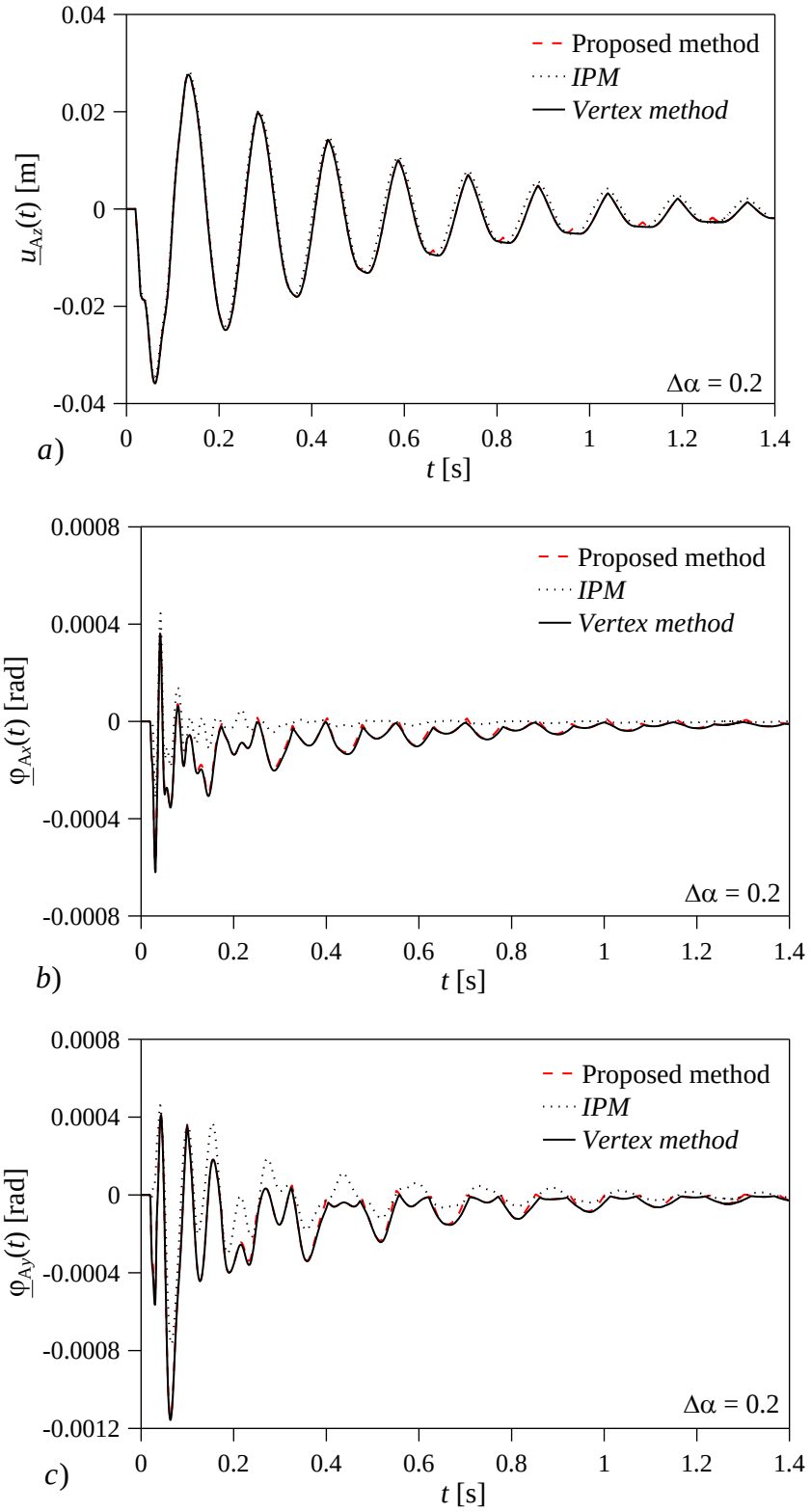


**Figure 7.** Time-histories of the *LB* of the interval a) displacement $u^I_{Az}(t)$ and rotations b) $\varphi^I_{Ax}(t)$, c) $\varphi^I_{Ay}(t)$ of node *A* of the grid structure provided by the proposed method, *IPM* and *vertex method*, for a deviation amplitude of the uncertain parameters $\Delta\alpha = 0.2$.

**Figure 8**

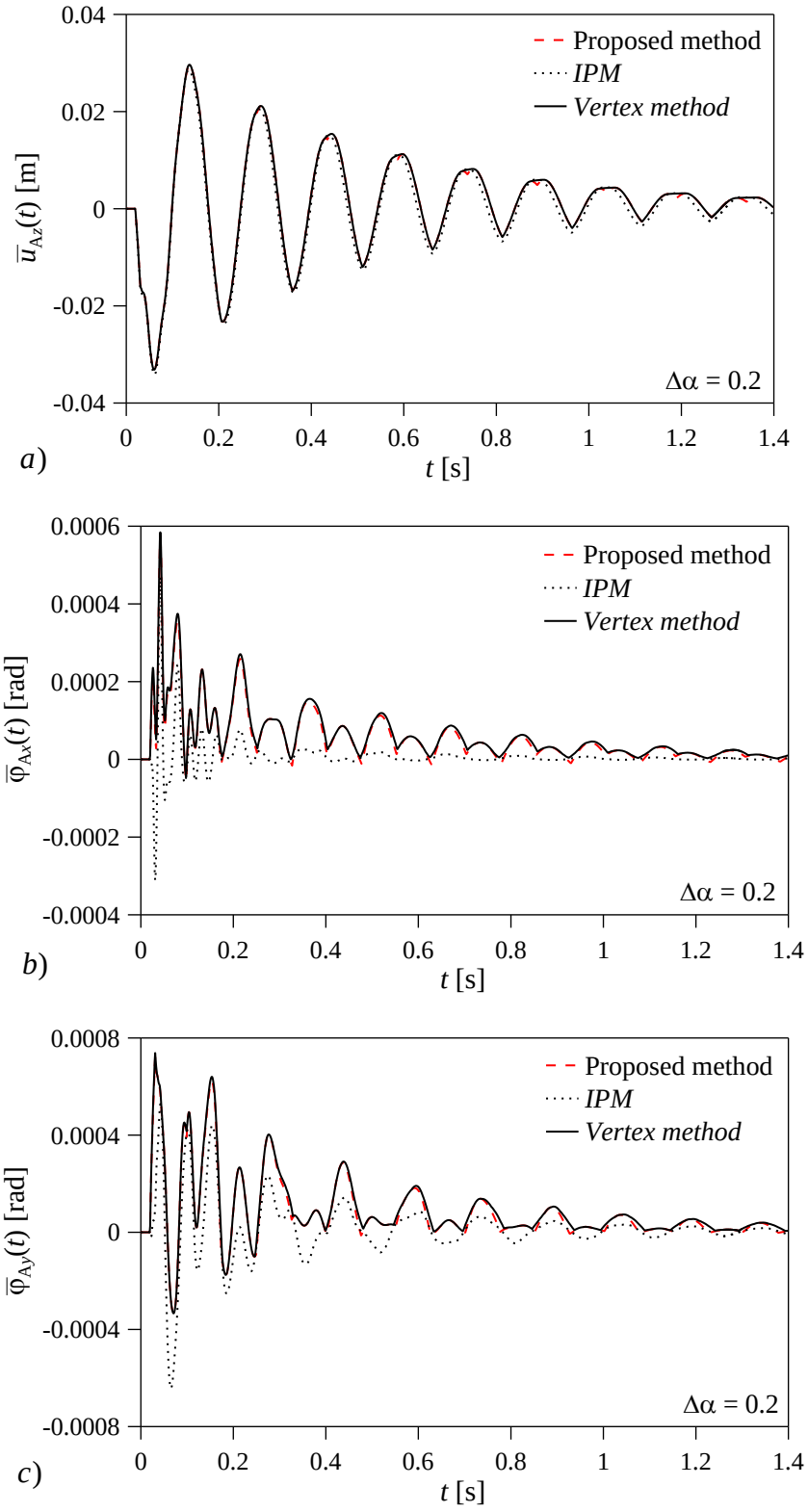


**Figure 8.** Time-histories of the *UB* of the interval a) displacement $u^I_{Az}(t)$ and rotations b) $\varphi^I_{Ax}(t)$, c) $\varphi^I_{Ay}(t)$ of node *A* of the grid structure provided by the proposed method, *IPM* and *vertex method* for a deviation amplitude of the uncertain parameters $\Delta\alpha = 0.2$.

**Figure 9**

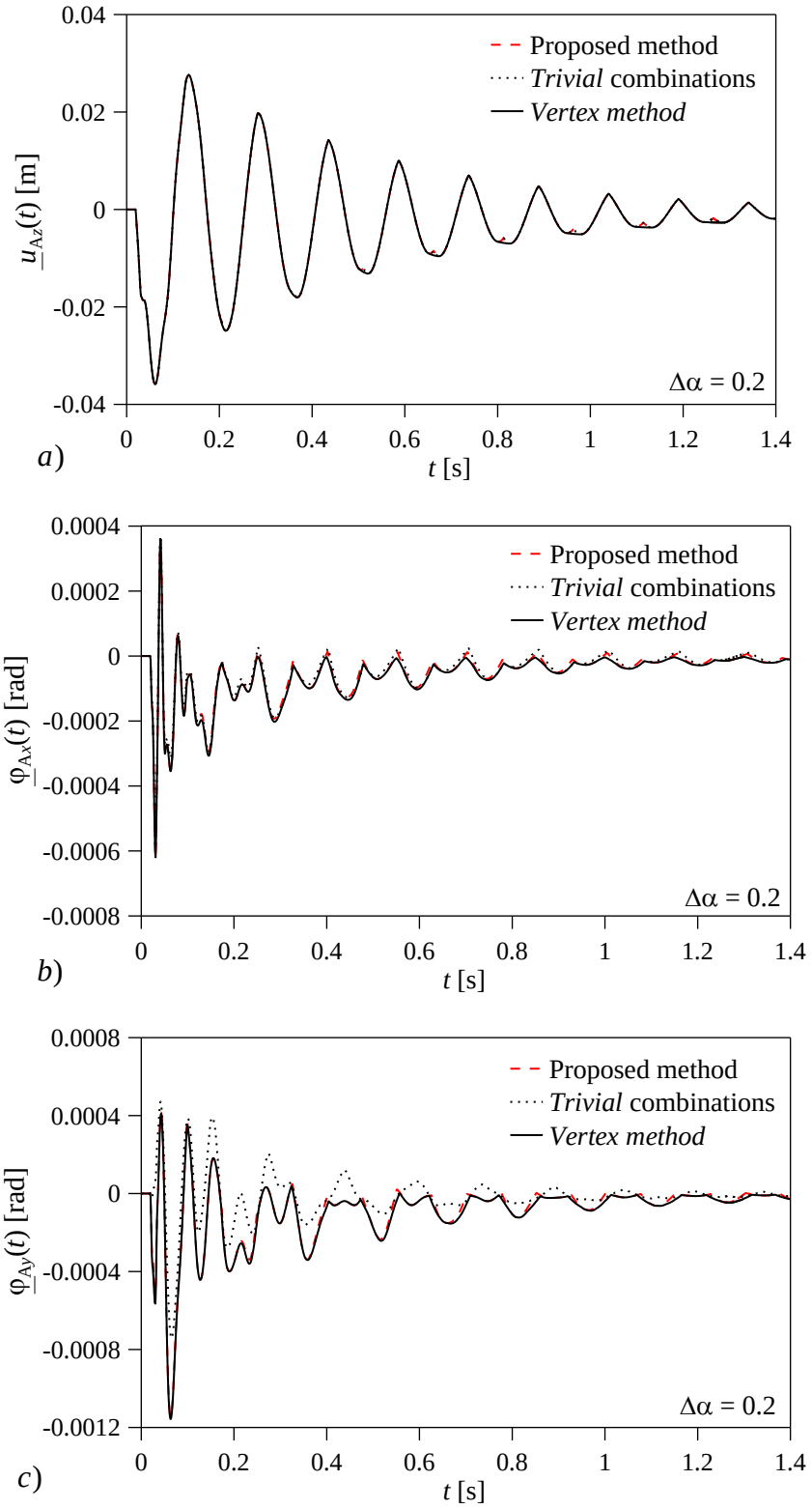


**Figure 9.** Time-histories of the *LB* of the interval a) displacement $u^I_{Az}(t)$ and rotations b) $\varphi^I_{Ax}(t)$, c) $\varphi^I_{Ay}(t)$ of node *A* of the grid structure obtained applying the proposed method, the *vertex method* and considering the *trivial* combinations of the endpoints of the uncertain parameters for $\Delta\alpha = 0.2$.

**Figure 10**

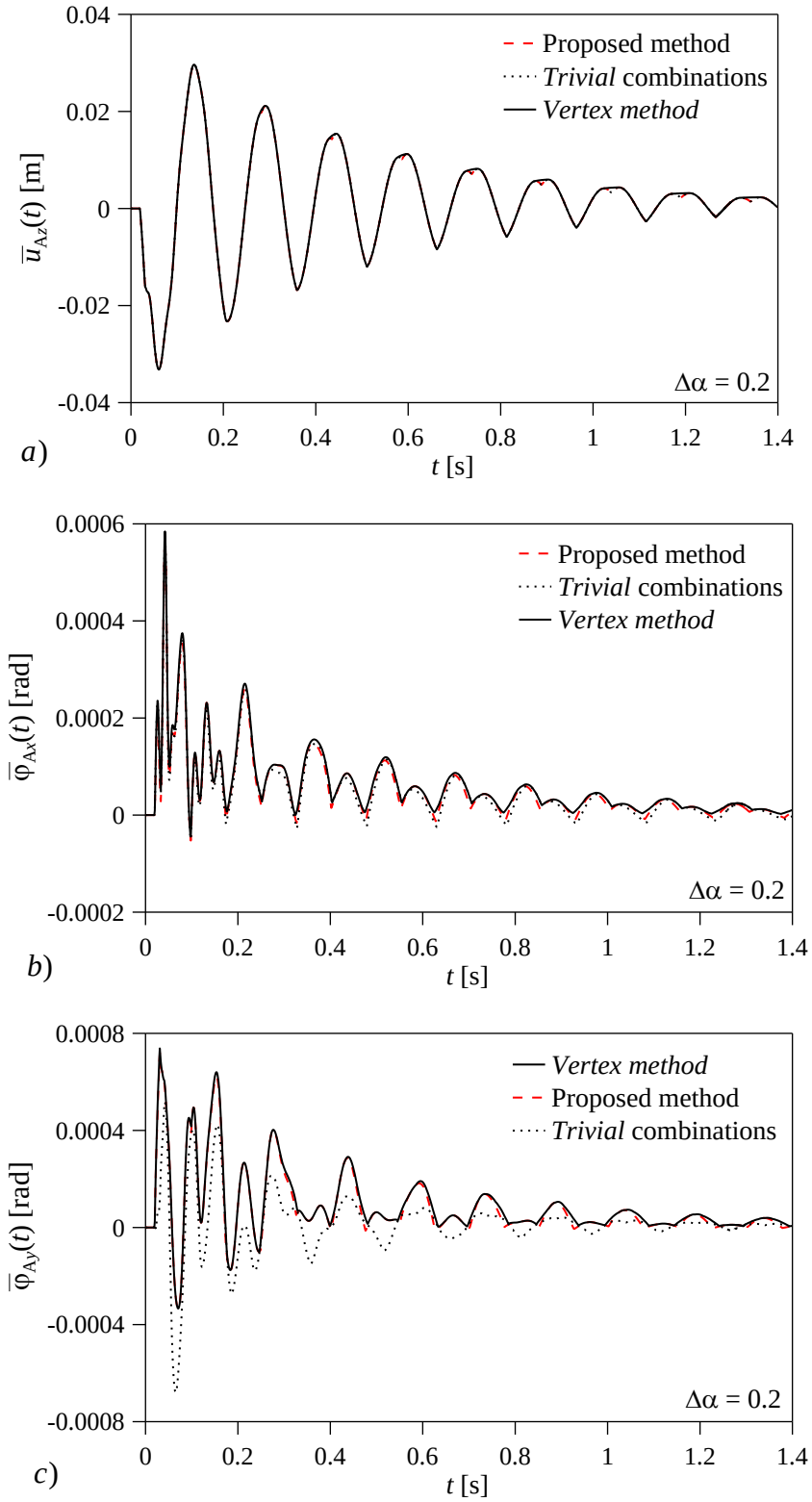


**Figure 10.** Time-histories of the *UB* of the interval a) displacement $u^I_{Az}(t)$ and rotations b) $\varphi^I_{Ax}(t)$, c) $\varphi^I_{Ay}(t)$ of node *A* of the grid structure obtained applying the proposed method, the *vertex method* and considering the *trivial* combinations of the endpoints of the uncertain parameters for $\Delta\alpha = 0.2$.

**Figure 11**

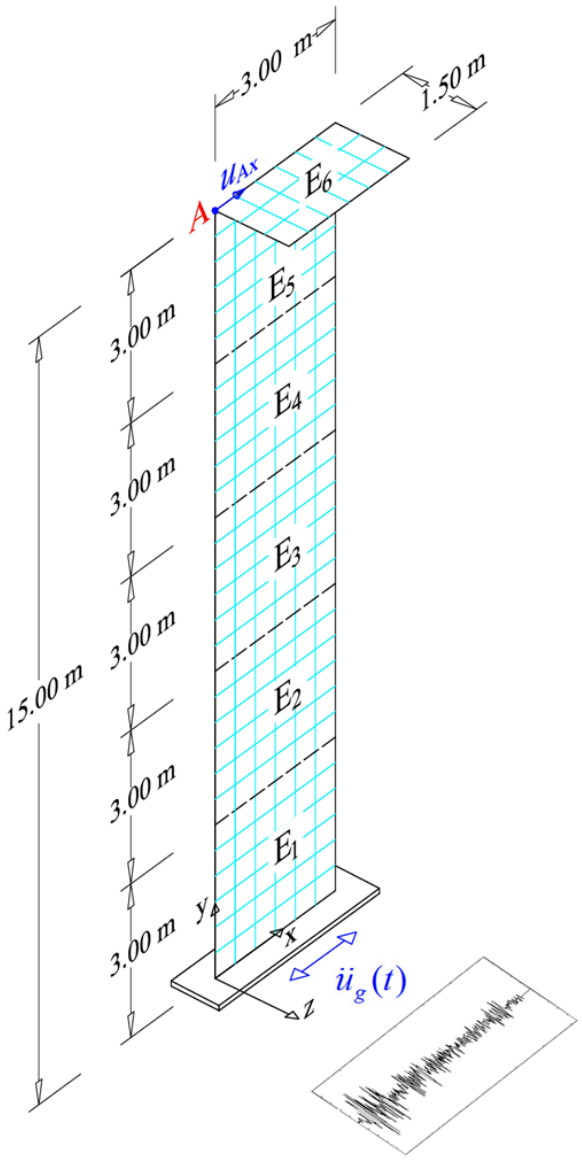


**Figure 11.** Shell corner with uncertain Young's moduli of $r = 6$ regions under El Centro ground motion acceleration along the $x-$direction.

**Figure 12**

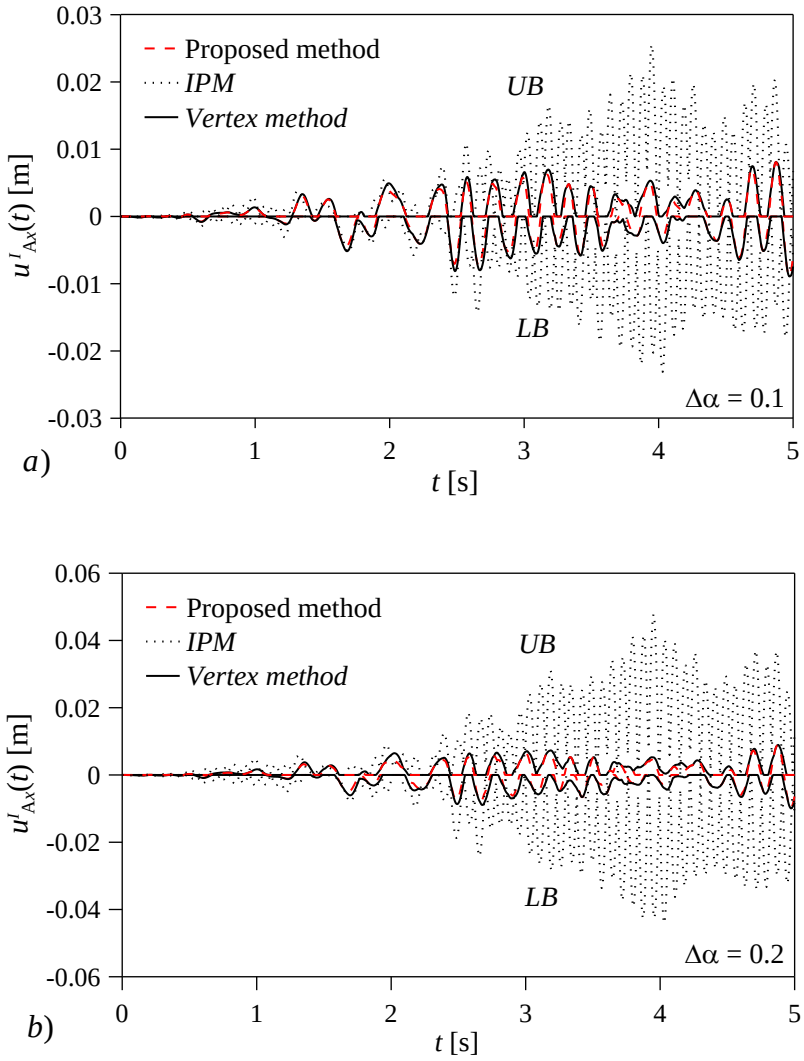


**Figure 12.** Time-histories of the *LB* and *UB* of the interval displacement $u_{Ax}^{I}(t)$ of the shell corner provided by the proposed method, *IPM* and *vertex method*, for a deviation amplitude of the uncertain parameters a) $\Delta\alpha = 0.1$ and b) $\Delta\alpha = 0.2$.

**Figure 13**

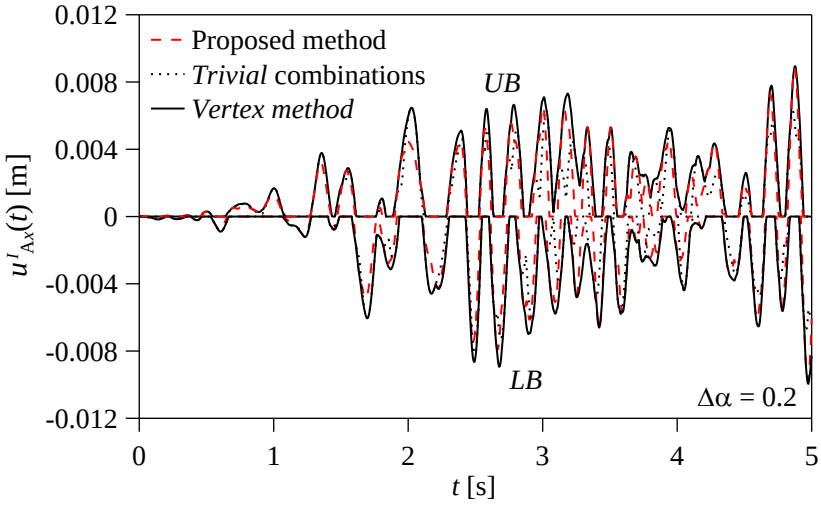


**Figure 13.** Time-histories of the *LB* and *UB* of the interval displacement $u_{Ax}^{I}(t)$ of the shell corner obtained applying the proposed method, the *vertex method* and considering the *trivial* combinations of the endpoints of the uncertain parameters, for $\Delta\alpha = 0.2$.